PIBB 生物化学与生物物理进展
Progress in Biochemistry and Biophysics
2018, 45(2): 148~169
www.pibb.ac.cn

Wolfgang Tremel received his Ph.D. in chemistry from the University of Münster under the guidance of B. Krebs. After short postdoctoral stays at the Hahn-Meitner Institute in Berlin and DESY/HASYLAB in Hamburg he joined the group of R. Hoffman at Cornell University as a postdoctoral research fellow (1984 –1986). He returned to Münster in 1987 to establish his own research. 1991 he moved to Johannes Gutenberg University as an associate professor and was appointed full professor in 1996. His research interests focus on the synthesis, structural and physical characterization and potential applications of new materials. One pillar of his research are inorganic nanoparticles with catalytic activity.

Leon Bixenmann received his Bachelor of Science degree in biomedical chemistry from the Johannes Gutenberg University Mainz in 2017. He finished his bachelor thesis in the group of Prof. K. Landfester at the Max Planck Institute. Now he is a Master student at the Johannes Gutenberg University Mainz and joined the group of Prof. X. Yan for a research semester abroad.

Functional Superoxide Dismutase Mimics Become Diverse: From Simple Compounds on Prebiotic Earth to Nanozymes

Leon Bixenmann[1)], Jiuyang He[2, 3)], Minmin Liang[2)], Wolfgang Tremel[1)*]

([1)] *Institut für Anorganische Chemie und Analytische Chemie, Johannes Gutenberg Universität, Mainz* 55128, Germany;
[2)] *Key Laboratory of Protein and Peptide Pharmaceuticals, CAS-University of Tokyo Joint Laboratory of Structural Virology and Immunology, Institute of Biophysics, Chinese Academy of Sciences, Beijing* 100101, China;
[3)] *University of Chinese Academy of Sciences, Beijing* 100049, China)

Abstract Inorganic solids with enzyme-like activity are promising to overcome many restrictions of native enzymes in application. Especially attractive are nanoparticles with superoxide dismutase (SOD) activity, due to their ability to reduce the damaging properties of reactive oxygen species within cells and organism. This review discusses the necessary requirements for nanoparticles to have SOD activity and reveals a close relationship between catalysis on prebiotic earth and the recent SOD mimics. This review also aims to highlight the progress in the development of SOD mimicking nanoparticles. We give a broad overview of nanoparticles with SOD activity, based on their material make-up, to underline their increasing diversity.

Key words nanozyme, SOD mimic, superoxide dismutase mimic, nanoparticle
DOI: 10.16476/j.pibb.2018.0040

* Corresponding author.
Tel: +49613139-25135, E-mail: tremel@uni-maiz.de
Received: January 25, 2018 Accepted: January 29, 2018

In cellular metabolism, oxygen undergoes a series of one electron reductions, leading sequentially to the formation of superoxide radicals $O_2^{\cdot-}$, hydrogen peroxide (H_2O_2), and H_2O. Reactive oxygen species (ROS) including free radicals, H_2O_2 and reactive metabolites such as $O_2^{\cdot-}$, are involved in the stimulation of signaling pathways in response to changes of external conditions and due to their high reactivity, they are a part of the inflammatory response to combat infections [1]. ROS can react with many important biomolecules including proteins, lipids or nucleic acid polymers (RNA and DNA) [2]. Therefore, enzyme systems like superoxide dismutase (SOD), glutathione peroxidase, and catalase that are responsible for protecting cells from the detrimental effects of ROS have evolved. Nevertheless, excessive ROS can be formed depending on the living conditions (ultraviolet radiation), health status (injuries, chronic infections, inflammatory disorders, nonsteroidal anti-inflammatory drugs), or lifestyle (cigarette smoking, alcohol) [3–5]. This can cause oxidative stress in living organisms and results in an imbalance between the formation of ROS which their elimination by protective mechanisms.

Research during the last decade has shown that oxidative stress can lead to diseases such as chronic inflammation and eventually to cancer, diabetes, cardiovascular, neurological and pulmonary diseases [6–11]. Since superoxide is a precursor of many other ROS, SOD enzyme has been considered as the first line of defense to treat these diseases. An SOD enzyme was even used as an antirheumatic drug, but the immunogenic reactions caused several cases of deaths and the drug was prohibited in Germany [12–13]. Despite the potential of recombinant enzymes, their shortcomings are obvious, including low biological availability and vulnerability to enzymatic degradation [14].

To overcome these challenges of recombinant enzymes, research has focused on the development of enzyme mimicking catalysts. Enzyme mimics in general are considered potentially low-cost and biocompatible alternatives. The first enzyme mimics probably existed even before enzymes evolved. On prebiotic earth, it is believed that simple inorganic mineral surfaces could have provided almost any type of general catalysis, but lacking substrate specificity or efficiency [15]. Similarly, many nano-sized inorganic solids exhibited enzyme-like activity. These nanoparticles (NPs), termed “nanozymes”, are highly promising because they have shown high catalytic ability when combined with their chemical properties. Some NPs can even cross the blood brain barrier, which is impossible for SOD enzymes [16–18]. Encouraged by these advantages, research focused on the development of new nanozymes. NPs with SOD like activity have shown promising results in a variety of applications, ranging from medicine development for the treatment of diseases, like cancer or neurodegenerative diseases or biosensing [16, 19–24], to industrial applications, for instance as an antioxidative additive in polymers or in cigarette filters to remove toxic superoxide anions [25–26].

Despite the tremendous progress in recent years, there are still many challenges to overcome like the low substrate specificity, limited catalytic reactions, and possible toxicity [16]. This review discusses the necessary requirements for SOD nanozymes and reveals a close relationship between catalysis in prebiotic earth and catalysis of recent SOD mimics. Further, the review aims to highlight progress in the development of SOD mimicking NPs. We give a broad overview of the NPs with SOD activity, based on their material-make-up, to underline their increasing diversity.

1 Evolution of enzymes

The first signs of life on earth appeared about 4.5 billion years ago. It is still not understood, how life arose. Deep sea hydrothermal vents have been suggested in addition to lightning-struck primordial soups or radioactive beaches. In any case, a series of events led to the evolution of membrane- bound cells with nucleic acids that were able to replicate.

Enzyme mimics may have played an important role as catalysts in the evolution of life in deep sea hydrothermal vents [27]. These vents have been suggested as the cradle of life. Hot hydrothermal vents release water that is heated by hot magma found in shallow chambers under the sea floor. In an other type of vent the water is superheated and forced back up to the sea floor. It contains minerals dissolved from the basalt ocean plate. A vent forms when the jet of water shoots through the sea floor and the dissolved minerals begin to precipitate. Hydrothermal vents can form black or white smokers, whose color depends on the type of minerals dissolved in the water [27]. Black smokers contain minerals with high levels of iron, manganese, copper, and zinc. White smokers release

minerals containing barium, calcium, and silicon. Several of these minerals have a high surface area-to-volume ratio and provide potential sites for heterogeneous catalysis [15]. The first NPs with enzyme-like activity (“nanozymes”) may have occurred in prebiotic life.

But how could prebiotic enzymes develop? The evolution of life from prebiotic soup *via* essential components to cells with a metabolism that allows a survival and reproduction of cells requires a complex network of enzyme-catalyzed processes. One feature that distinguishes cells from their presumed early precursors is the evolution of metabolic pathways. Many enzymes catalyze transformations between compounds that are needed only for a part of a specific metabolic pathway and not essential for other functions of the cell. Thus, it is unlikely that enzymes involved in the formation of intermediates of a metabolic pathway evolved without the end products in place.

It is assumed that in the early days of evolution metabolism needed only a small number of enzymes with low effectiveness and broad specificity. These enzymes become more specialized and effective *via* natural selection, and the broad specificity of many representatives has been lost. A second generation of enzyme evolution could have started from pre-existing enzymes that already had reasonable specificity and efficiency.

The current explanation of enzyme evolution is based on two models [28], the *retro-evolution* model [29] and the *recruitment model* [30]. The *retro-evolution* model [29] assumes that cells employed initially useful metabolites from the environment. When one of the metabolites became depleted, the cell developed an enzyme that converted a related compound, available in the environment, to the depleted metabolite. The complete biosynthetic pathway developed simply by repetition of this procedure. The depletion of the intermediate could be modest, and the efficiency of the new enzyme could be modest at the initial stage. A slight depletion in the concentration of an essential metabolite may have been sufficient to change the growth rate of a cell. Thus, even an inefficient enzyme would have been sufficient to replace a previous one after several generations.

Many protein classes were present before the key elements of the protein synthesis apparatus were developed. Assuming that a *de novo* evolution of new enzymes is unlikely under selection pressure, one key question in the evolution of a metabolic pathway is how an existing enzyme could be recruited to perform a new task [30]. The *recruitment model* of enzyme evolution proposes that enzymes evolve by duplication and mutation of similar enzymes from other pathways. A single recruitment mechanism is unlikely because of the complexity of metabolic pathways and the need for alternatives under different environmental conditions — considering also different genetic resources available for a given species at a time.

Primitive cells may have contained only a few enzymes, catalyzing reactions with broad substrate specificity. These enzymes then may have been recruited for new metabolic pathways, while more specific and efficient catalysts could have developed later. Therefore, “proto-enzymes” may have been multifunctional in the early stages. Nanoparticle-based enzyme mimics are prototypical examples of multifunctional catalysts. Cerium dioxide (ceria, CeO_2) NPs have been reported to have peroxidase, superoxide dismutase (SOD), catalase and phosphatase properties, i.e. they have oxidoreductase and hydrolase properties [31–35]. This multifunctionality may have been relevant when respiration turned from anaerobic to aerobic, because respiration was completely anaerobic when life on earth began[36].

The atmosphere contained mostly carbon dioxide and methane. Redox pathways with cycles of electron donors and acceptors had to develop to produce energy that powered cellular processes. The main electron donors were initially H_2, H_2S and CH_4, and the main acceptor probably nitrogen. Water, the electron donor for photosynthesis, was abundant, but there was still no biochemical mechanism for water splitting, and it remained unused. When the CO_2 levels decreased, methane levels went up and the planet warmed up due to global warming. When photosynthesis developed, carbon dioxide could be converted to useful sugars, but photosynthesis also produced oxygen as toxic waste product, until enough free molecular oxygen accumulated on the atmosphere. The oxygen led to a failure of the internal redox potentials in cells, formed dangerous free-radicals and precipitate ions out into insoluble forms, thereby killing the majority of life until organisms developed systems to handle oxygen efficiently and use it for aerobic respiration.

Aerobes survive in the presence of oxygen only by virtue of an elaborate defense system. Without

defense, organisms die because key enzyme systems in the organisms fail. Obligate anaerobes, which live only in the absence of oxygen, do not possess the defenses that make aerobic life possible and therefore do not survive in air.

In cellular metabolism, oxygen undergoes a series of one electron reductions, leading sequentially to the formation of $O_2^{\bullet-}$, hydrogen peroxide (H_2O_2), and H_2O. Enzymatic sources of reactive oxygen species (ROS) are components of the mitochondrial electron transport chain, xanthine oxidase, the cytochrome P450 monooxygenases, lipoxygenase, nitric oxide synthase, and the NADPH oxidase. Singlet oxygen is very reactive. Therefore, superoxide ($O_2^{\bullet-}$) must be removed by dismutation to H_2O_2 with SODs, to allow a survival of the cell in the presence of oxygen. H_2O_2 is still an oxidant, but can diffuse out of the cell and is thus not as harmful as the superoxide anion. H_2O_2 is eliminated subsequently with the aid of catalase, peroxiredoxins, or glutathione peroxidases.

Facultative and aerobic organisms lacking SOD often have high concentration levels of catalase or peroxidase. This mitigates the need for SOD, because both enzymes scavenge H_2O_2 before it reacts with superoxide to form the highly reactive hydroxyl radical. The SOD activity and resistance to the toxic effects of oxygen is connected in many organisms. Facultative and aerobic organisms show high concentration levels of SOD. The enzyme occurs at lower concentration levels in some anaerobes, but the most oxygen-sensitive organisms contain little or no SOD. In addition, the reaction rate of organisms with oxygen is crucial for oxygen tolerance. Tolerant (facultative) organisms can process small amounts of oxygen or they show high SOD activity, anaerobes without SOD activity are killed by exposure to oxygen.

2 Basic requirements of functional SOD enzyme mimics

The oldest SOD mimic is the Mn^{2+} ion [37–39]. In *Lactobacillus plantarum* it can even replace the essential native SOD enzyme [40]. Barnese *et al*. demonstrated that the catalytic activity of manganese carbonate and manganese phosphate is high enough to replace the native enzyme[38–39]. But why are manganese carbonate and phosphate SOD mimics? It should be possible to define the required properties in a more general way. Although it may be difficult to describe the properties of all SOD mimics comprehensively, the basic requirements and rules can easily be summarized.

2.1 Functional SOD mimics — general reaction mechanism

One requirement for SOD activity is that the metal catalyst can shuttle in one-electron steps between two oxidation states. The reaction is catalyzed either by transition metal compounds or the native SOD enzyme. The respective catalyst metal is reduced in a one-electron transfer step, while a superoxide radical is oxidized to molecular oxygen in return. In the second step the reduced catalyst is re-oxidized by reducing a second superoxide radical to hydrogen peroxide. The reaction mechanisms are shown in Figure 1.

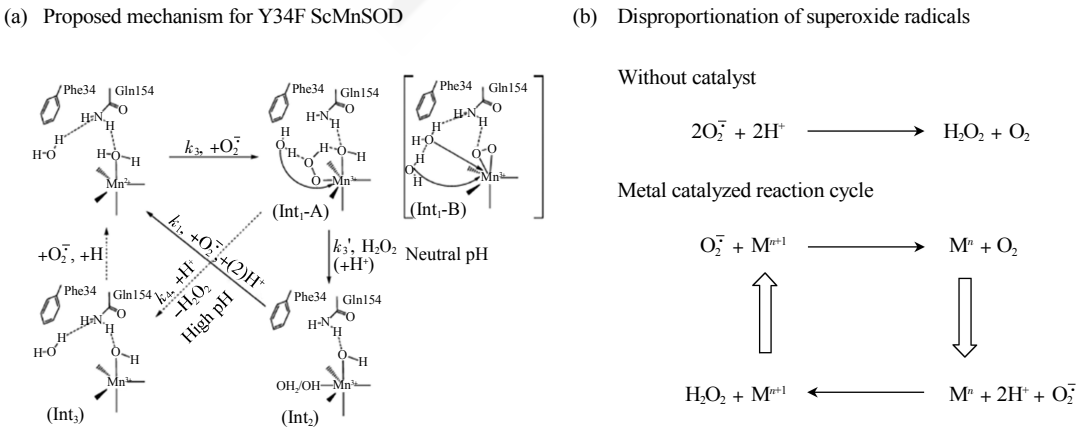

Fig. 1 Reaction mechanism of the disproportionation of superoxide radicals

(a) Proposed reaction mechanism for Yeast 34F ScMnSOD. Reproduced with permission from ref. [41]. (b) General reaction of the disproportionation of superoxide radicals. Superoxide radicals disproportionate to oxygen and hydrogen peroxide. Metal catalysts catalyze the reaction by shuffling between two oxidation states.

2.2 Functional SOD mimics — thermodynamic aspects

The choice of the possible catalysts is limited by the redox potential. With the reduction potentials $E(O_2/O_2^{\cdot-}) = -0.16$ V and $E(O_2^{\cdot-}/H_2O_2) = +0.94$ V (for standard conditions, pH 7) of the two half-reactions, the redox potential E_m of the metal catalyst should lie in between these two values to promote both half-reactions reversibly, *i.e*. the reduction potential of the metal should be ideally ≈0.36 V (for standard conditions, pH 7) [42-43]. This concept is supported by the reduction potentials of different native SOD enzymes. Mn-SOD, CuZn-SOD, and Ni-SOD have reduction potentials close to 0.3 V (Figure 2) [43]. Moreover, a mutation in the second sphere amino acid in Fe-SOD, which increases the reduction potential by 0.24 V, leads to the enzymatic activity decrease of 66% [44]. While the reduction potential of the Mn^{3+}/Mn^{2+} redox pair (aqua complexes) precludes any SOD activity [45], enzyme-bound Mn^{2+} or manganous phosphate or carbonate are efficient SOD mimics [38, 46], because Mn^{2+} complexation (SOD enzymes) or precipitation (manganous phosphate, manganous carbonate) shift the redox potential to lower values through the concentration term of the Nernst equation [47]. By addition of $NaHCO_3$ to $MnSO_4$, the reduction potential decrease by more than 0.5 V (compare Figure 2).

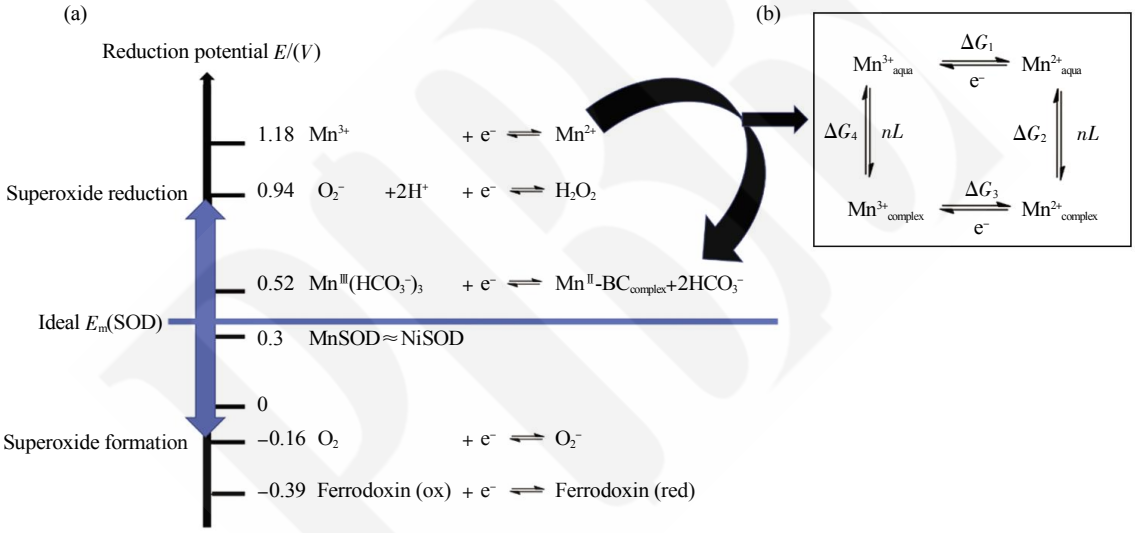

Fig. 2 (a) Ideal reduction potential for superoxide dismutase mimicking catalysts. While the reduction potential of the Mn^{3+}/Mn^{2+} redox pair (aqua complexes) precludes any SOD activity, (b) Mn^{2+} complexation (SOD enzymes) or precipitation (manganous carbonate) shift the redox potential to lower values [47]. This enables (from a thermodynamic prospective) SOD activity.

The range of the reduction potentials of metal ions for possible superoxide dismutation catalysis is shown as a blue arrow. Native SOD enzymes have reduction potentials close to the ideal E_m value. Ferredoxins are located inside the mitochondria. Their low reduction potential (ferredoxin (red)) allow the reduction of oxygen to superoxide. (ox = oxidized / red = reduced). Reference: native SOD enzymes ref: [43]; ferredoxin, cytochrome c (at pH 7) ref: [48], Mn^{3+}/Mn^{2+}, $Mn^{III}(CHCO_3^-)_3/Mn^{II}$-$BC_{complex}$ (Mn^{II}-$BC_{complex}$ represent the a manganous carbonate complex or cluster, which structure wasn't determined): (reduction potential was determined in a solution with the concentration $c(MnSO_4) = 5 \times 10^{-5}$ mol/L and $c(NaHCO_3) = 40 \times 10^{-3}$ mol/L) ref: [47], $O_2/O_2^{\cdot-}$, $O_2^{\cdot-}/H_2O_2$.; pH 7 ref: [49]. Thermochemical cycle of the complexation on the redox potential, illustrating the modulating effect of ligands (L) or precipitation on the standard reduction potential of manganese ions. The difference in free energy is abbreviated as ΔG. The complexation effect on the redox potential is reviewed by Rizvi[50].

The close relationship between the reduction potential and the SOD activity is illustrated in Figure 3. Although the data in Figure 3 are based on those for molecular manganese complexes, a similar activity trend may be expected for the NPs, where the Mn concentration is defined by the solubility product of the catalyst, because a sufficient thermodynamic driving force is a universal concept.

We conclude that for all SOD enzymes and enzyme mimics (ⅰ) the metals must be able to shuttle between two oxidation states and (ⅱ) the reduction potential dictates the activity of the catalyst.

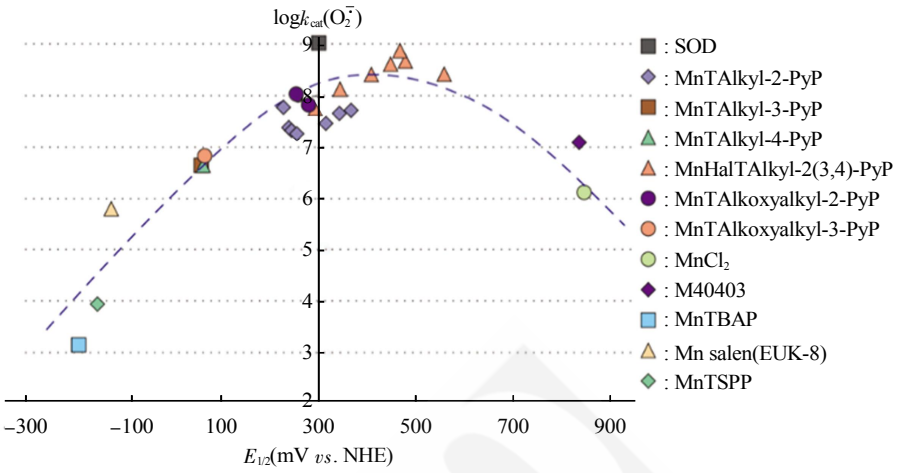

Fig. 3 Superoxide activity as a function of the reduction potential for different manganese containing compounds (superoxide activity expressed as the logarithm of the reaction rate constant for the disproportionation of superoxide radicals)

Reproduced with permission from ref. [51].

2.3 NPs as functional SOD mimics — general principles from heterogenic catalysis

The catalytic reaction cycle can be roughly divided into several reaction steps. The substrate is first adsorbed on the catalyst surface, then the adsorbed species undergo reaction, and the final products must be desorbed from the catalyst. Although this description is simplified as it neglects the effects like surface reconstruction, surface layer formation, and the diffusion process into sub-surface regions, it has been used to develop an understanding of trends in transition-metal catalysis: scaling relations, activity maps, and the *d*-band model. Scaling relations correlate the surface bond energies of adsorbed substrates (also including possible transition states). This maps the manifold of reaction variables responsible for the rate of a catalytic reaction onto a handful of descriptors. The result is an activity map, which shows a semi-quantitative implementation of the Sabatier principle, one of the oldest qualitative concepts in catalysis [52]. It states that there is an optimum "bond strength" for the best catalyst for a given reaction (Figure 4a), as metal-adsorbate bonding is accomplished at the expense of bonding within the metal and within the adsorbent molecule. The scaling relations define the relevant "bond strengths". The descriptors can be measured (or calculated) and used to set up a reaction model, which permit the "tuning" of a catalyst. In the next step, the model can be tested experimentally by making predictions for improving the catalyst. The *d*-band model provides an understanding of the scaling relations and variations in catalytic activity in terms of the electronic structure of the transition-metal surface [53].

The adsorption energy depends not only on the catalyst composition, it may also change dramatically from different surfaces. As an example, Peter *et al*. studied the correlation between the oxygen adsorption energy on Pd NPs and the particle size *in vacuo* [54]. There are two opposing effects, which influence the adsorption energy of oxygen (Figure 4b). The number of unsaturated sites increases with a decreasing particle size (Figure 4c). On the other hand, the adsorption energy decreases with decreasing particle size (Figure 4d), because for very small particles with only a few atom layers the buffer effect of the sub-surface layers will be exhausted and electrons for substrate bonding are no longer available. An essential requirement for heterogeneous catalyst is that the active site is accessible for chemisorption from the reaction environment [52]. When the catalytic site of an enzyme is blocked, the enzyme is inactivated. For NP enzyme mimics, *i.e*. in the heterogeneous case, the surface atoms must have vacant coordination sites

available for substrate binding. Surface defects like steps, kinks, adatoms, or vacancies are coordinatively unsaturated and therefore reactive [52]. Figure 4 explains the different nano size-effects, which influence the properties of NPs and which are related to the catalytic properties of nanozymes. Figure 4c reveals that at a specific particle size the relative amount of edge sites increase drastically. In this case at a particle size of 1 nm almost 80% of the atoms are edge site atoms, which influence their catalytic properties drastically. The reaction mechanism of nanoceria as an SOD mimic is a very illustrative example for the importance of defects in nano-catalysis (Figure 5).

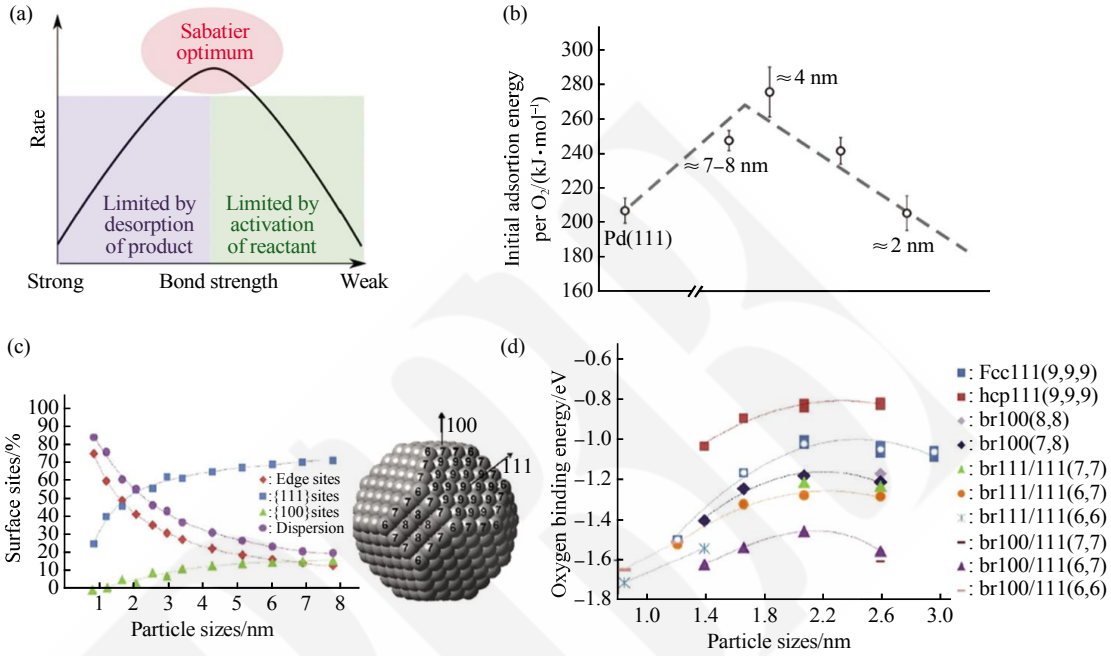

Fig. 4 General principles for heterogenic catalysis

(a) Vulcano plot and Sabatier optimum.(b) Size dependence of the initial adsorption energy per O_2 molecule on a Pd{111} surface. (c) Calculated ratio between the number of surface site atoms and the overall number of atoms in a truncated octahedral platinum Np as a function of particle size. (d) Oxygen binding energy as a function of particle size for difference surface sites and coordination numbers, calculated by using density functional theory for platinum NP. Reproduced with permission from ref: (a), [55], (b), [54], (c) and (d), [56].

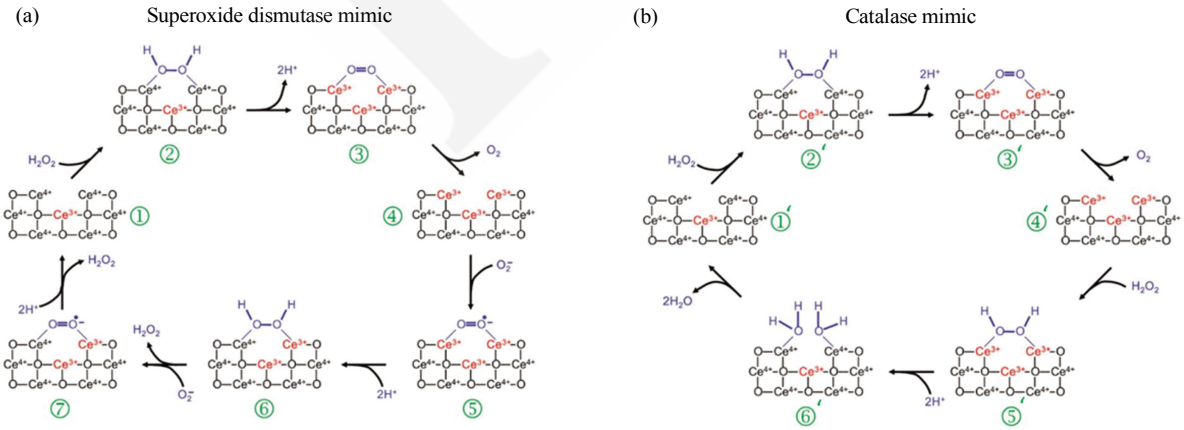

Fig. 5 Proposed reaction mechanism for nanoceria catalyzing (a) the disproportionation of superoxide and (b) hydrogen peroxide

(a-1) Oxygen vacancies on the CeO_2 surface. (a-2) H_2O_2 binds to the defect site. After deprotonation, two electrons are transferred that reduce 2 Ce^{4+} sites to Ce^{3+}. (a-3) Oxygen is released from the vacancy and (a-4) replaced by a superoxide anion. (a-5) After protonation of the surface-bound superoxide one electron is transferred for the formation of surface-bound H_2O_2, (a-6) which is released and replaced by a second superoxide anion. (a-7) In a next reduction step the second superoxide anion is reduced to H_2O_2, which is relased and the initial state is restored. (b-1) Oxygen vacancies on the CeO_2 surface. (b-2) H_2O_2 binds to the defect site. After deprotonation, two electrons are transferred that reduce 2 Ce^{4+} sites to Ce^{3+}. (b-3) Oxygen is released and (b-4) the vacancy is (b-5) saturated with a H_2O_2 molecule (b-6) after 2-fold protonation the O-O bond is split and 2 water molecules are released. This restores the initial state (b-1). Reproduced with permission from ref. [32].

Conclusions from the principles of heterogenous catalysis for NP SOD mimics are: (ⅰ) The binding of the reactants should not be too strong to prevent the irreversible reactions, but strong enough to activate the substrates for the subsequent reactions. (ⅱ) Particle size, surface energy and surface defects are important variables for the reactions, and (ⅲ) coordinatively unsaturated surface sites must be accessible for chemisorption. Nanoceria is the most frequently studied nanoparticle SOD mimic. In the sequel, we will discuss the reactions of nanoceria in the light of the requirements introduced before.

3 Nanomaterials with SOD-like activity

3.1 Cerium dioxide as a functional SOD mimic

Cerium dioxide is widely used in industry as a catalyst, for instance in automobile exhaust systems[57]. Recently it has been found that Ceria NPs(CeO_{2-x}) can mimic an abundant of enzymes, including SOD, phosphatase, peroxidase, oxidase and catalase and they gained increasing interests in recent years [31–35, 58]. Especially, their high superoxide scavenging activity, when combined with their good biocompatibility and low toxicity, is outstanding [24, 32, 59]. The high biocompatibility of CeO_2 and the low environmental toxicity can partially be explained by the insolubility of CeO_{2-x} in water. Due to these reasons the catalytic ability of nanoceria has recently been well studied as SOD mimicking nanozymes, which will be discussed in the next paragraph.

3.1.1 Reaction mechanism of nanoceria mimicking SOD and catalases

Nanoceria have been found to mimic several enzymes such as SOD, catalase, phosphatase and oxidase [31–34]. Celardo *et al.* proposed a plausible mechanism for the SOD and catalase reaction on the nanoceria surface, which is based on the shuttling of cerium between its Ce^{3+} and Ce^{4+} oxidation states [32]. This can partially be explained by the similar energies of the 4f and 5d electronic states (giving rise to mixed configurations in solid state compounds) [57]. The surface of nanoceria, contains oxide vacancies associated mainly with the presence of Ce^{3+} and Ce^{4+}, but also with the large number of defects for small NPs[2, 57, 60] (Figure 6). Ce^{3+} species are present mainly on the surface sites, because the ionic radius of Ce^{3+} is incompatible with the fluorite lattice. Charge neutrality requires the presence of 1/2 equivalents of oxide for each Ce^{3+} site, as described by the Kröger-Vink notation $2\,Ce^{x}_{Ce} + O^{x}_{O} = 2Ce'_{Ce} + V^{\cdot\cdot}_{O} + 1/2O_2(g)$, where Ce'_{Ce} indicates the formation of a Ce^{3+} defects on Ce^{4+} lattice sites and $V^{\cdot\cdot}_{O}$ shows the formation of a doubly ionized oxide vacancy and 1/2 O_2 (g) the release of 1/2 equivalent of molecular oxygen[61].

It is established that the oxide vacancies are significant for the catalytic properties of nanoceria. The number of oxygen vacancies increases with a decreasing particle size [57, 60]. Size and surface properties of ceria NPs strongly affect their reactivity. Depending on the Ce^{4+}/Ce^{3+} ratio, either catalase or SOD activity prevails [2, 24, 62]. Comprehensive reviews about the defect structure of nanoceria have been published[57, 61].

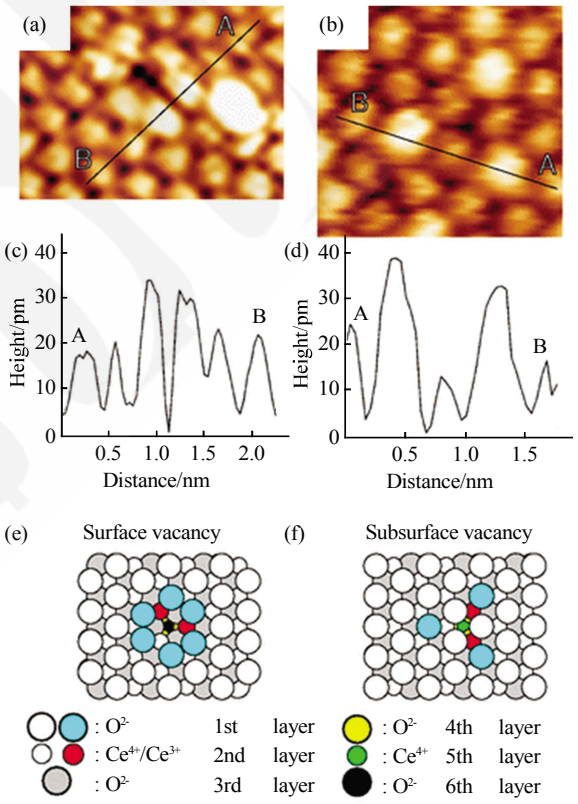

Fig. 6 Oxygen vacancies on a ceria surface

Dynamic mode atomic force microscopy (*DFM*) *image* displaying the *topography* of a surface (a) and a subsurface (b) oxide vacancy, together with the corresponding height profiles (c) and (d) and the associated structural models (e) and (f), respectively. The protrusion at the right side of the surface oxide vacancy (a) is attributed to a hydroxide group substituting a surface oxygen atom. Reproduced with permission from ref. [63].

3.1.2 An illustrative example: Ceria NPs for treatment of neurodegenerative diseases

A high percentage of earth population suffers

from neurodegenerative disorders. In the United States, ischemic stroke is one of the main causes of adult long-term disability [64]. During cellular respiration in aerobic mitochondria, oxygen is reduced to water in a one-electron reduction steps. This process leads sequentially to the formation of $O_2^{\cdot-}$ and H_2O_2 intermediates and eventually to H_2O. In several neurodegenerative diseases, additional ROS is generated. This increased oxidative stress can damage cells irreversibly or lead to apoptosis [65]. Nanoceria-based protection against oxidative damage is based on the ROS scavenging properties and biocompatibility. Most NPs cannot penetrate the intact blood-brain barrier (BBB), but in the case of diseases (such as ischemic stroke) the BBB gets leaky and NPs may can cross [20]. Many groups studied the neuroprotective effects of nanoceria [19-20, 66-69]. Chen and coworkers reported that an intravitreal injection of nanoceria particles protect rat retina photoreceptor cells from photo-induced damage [19]. Later in an ischemic stroke animal model nanoceria decreased the ROS-induced damage in rat and mouse brain [20, 70].

Alzheimer's disease (AD) is the most common reason for dementia [71]. In 2015, already 46.8 million people suffer this disease, a trillion of dollars is expected as the worldwide cost of dementia in 2018 [72]. Nevertheless, there is still no satisfactory prophylaxis or useful therapy. The mechanism of Alzheimer's disease is still not completely understood. In the brains of Alzheimer patients, amyloid plaques were observed, and a polymerization of amyloid-β peptide (Aβ) into amyloid fibrils (plaques) is believed to be related to its pathogenicity. Oxidative stress and metal dysregulation have been proposed as therapeutic targets for AD, the metal ions playing a significant role in Aβ aggregate disposition and neurotoxicity [73]. High levels of metal ions also catalyze ROS formation *via* the Fenton reaction. To protect the affected cells, ceria NPs were coated with 1,2-distearoyl-*sn*-glycero-3-phosphoethanolamine-N-[amino (polyethylene glycol)] with a triphenylphosphonium cation at the PEG terminal (DSPE-PEG-TPP) [65]. This lipophilic cation targets mitochondria because of the negative mitochondrial membrane potential. Although, these NPs didn't eliminate subicular Aβ deposition significantly, they were able to reduce oxidative stress in mitochondria *in vitro* (compare Figure 7) [65]. Furthermore, *in vivo* study on Alzheimer mice model, provided evidence that this NP can restore neuronal viability.

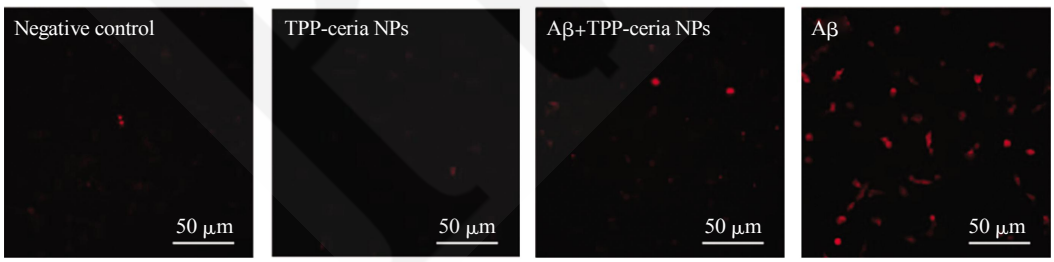

Fig. 7 TPP-coated ceria NPs significantly inhibit Aβ-induced mitochondrial ROS in vitro

Confocal fluorescence images of mitochondrial ROS accumulation in U373 cells obtained with a superoxide detection reagent. U373 cells untreated (negative controls), exposed to 0.1 mmol/L TPP-ceria NPs (TPP-ceria NPs), to 5 μmol/L Aβ and 0.1 mmol/L TPP-ceria NPs (Aβ + TPP-ceria NPs), and to 5 μmol/L Aβ (Aβ) for 12 h. Reproduced with permission from ref. [65].

Inspired by a previously developed proteolytic polyoxometalate based gold NPs with SOD activity, Yijia Guan *et al*. designed a ceria/polyoxometalate hybrid (CeO_2/POMD) NPs which exhibits radical scavenging and proteolytic ability to remove Aβ aggregates [67-68]. When Aβ aggregates are exposed to cells, their ROS levels increase. Pretreatment of cells with ceria (before Aβ aggregate exposure) decrease the ROS levels by 35% while ceria/POMD diminished them by 68%. The proposed proteolytic mechanism is shown in Figure 8. *In vivo* studies with mice indicated a good biocompatibility, after 24 h of a single dose injection of NPs no tissue damage was observed.

A release system based on mesoporous silica

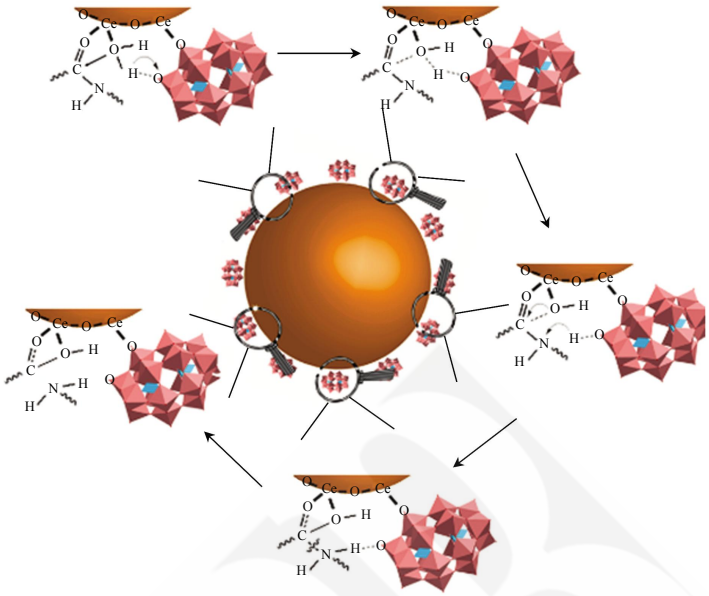

Fig. 8 Proposed proteolytic mechanism of ceria/polyoxometalate hybrid

Cerium ion interacting with the carbonyl group of proximal amide bond. This result in polarization and makes the carbon atom more susceptible to nucleophilic attack by water molecules. Reproduced with permission from ref. [68].

particles and glucose coated-CeO_2 NPs combines the anti-aggregation property of metal chelators and the anti-oxidation property of CeO_2 NPs on a single platform for Alzheimer's disease treatment [69]. Ceria capped the mesoporous silica pores by a covalent binding between the phenylboronic acid and the vicinal diols of glucose. In the presence of H_2O_2, the arylboronic esters are oxidized to phenols, and the mesoporous NP releases 5-chloro-7-iodo-8-hydroxyquinoline and ceria. Compared with metal chelators or CeO_2 NPs alone, a synergistic effect was observed in the H_2O_2 responsive controlled release system[69]. By using the biocompatibility, their ability to decrease cellular ROS and the efficient release of metal chelators, the two-in-one bifunctional NP system inhibits Aβ aggregate formation and protects cells from Aβ-related toxicity [69]. These findings are encouraging for the application of nanoceria for the treatment of neurodegenerative disorders.

3.2 Platinum-containing SOD mimics

Kajita *et al*. first reported the superoxide and hydrogen peroxide scavenging properties of Pt NPs, but the mechanism remained unclear. The NP system was a Pt-Au alloy with particle diameters in the range from 3 nm to 10 nm[74]. Later it was shown that Pt NPs increased the lifespan of the nematode *Caenorhabditis elegans* [75]. Based on density functional theory (DFT) calculations for the adsorption of O_2 on noble metal surfaces (*in vacuo*), Shen *et al*[76]. suggested a reaction mechanism for the SOD activities of noble metal (Au, Ag, Pt, Pd and their alloys) NPs. The catalytic activity critically depends on (ⅰ) the metal composition and (ⅱ) the exposed facets. The model proposes the protonation of $O_2^{\cdot-}$ and the adsorption and rearrangement of $HO_2^{\cdot}$ on the metal surface to be the most relevant factors. Since $O_2^{\cdot-}$ is a Brönsted base with a pK_b of 9.12 it can readily be protonated by water to form $HO_2^{\cdot}$. The calculations for the subsequent adsorption on the Pt {111} facet indicates an exothermic process, which shifts the equilibrium to the product side. Due to the low activation energy, they can efficiently react to O_2^* and $H_2O_2^*$, once they are adsorbed on the surface (Figure 9). The dissociative adsorption mechanism of O_2 sheds light on the activation of molecular oxygen by nanosurfaces to understand the role of metal nanocrystals as pro- and antioxidants.

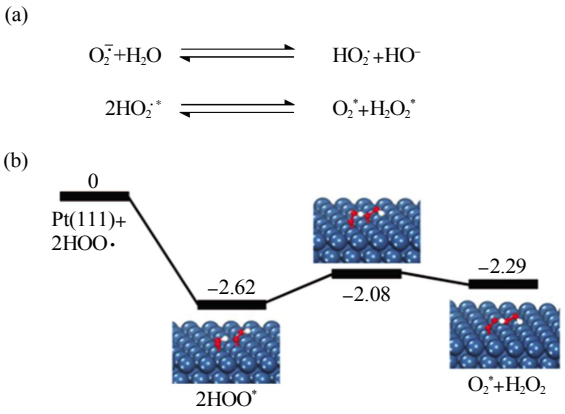

Fig. 9 Proposed reaction mechanism of the catalyzed disproportionation of superoxide radicals

(a) Protonation of $O_2^{\bullet-}$ and the adsorption and rearrangement of $HO_2^{\bullet}$ on the metal surface. (b) Potential energy profiles for the rearrangements of two $HO_2^{\bullet}$ groups on {111} facets of Pt. Reproduced with permission from ref. [76].

Apo-ferritin itself has been shown to have both catalase and SOD activity[77]. In an innovative approach, Pt NPs were encapsulated to combine their ROS scavenging ability while increasing their biocompatibility. This led to a selective receptor-mediated internalization of Pt NPs, which further prevented membrane damage by direct uptake (Figure 10). A concentration of 2.5 g/L Pt-apo show a minimal vitality loss of 2% in intestinal Caco-2 cells, while 417 mg/L Pt-apo already showed more than 60% of SOD activity [77].

In general, a dual SOD/catalase mimic is a significant advantage, because in the defense reaction for superoxide, hydrogen peroxide is formed. If the catalase activity cannot compete with the enhanced formation of hydrogen peroxide, it accumulates in cells. H_2O_2 leads to cell damage cause a variety of diseases. As a consequence, superoxide and H_2O_2 have

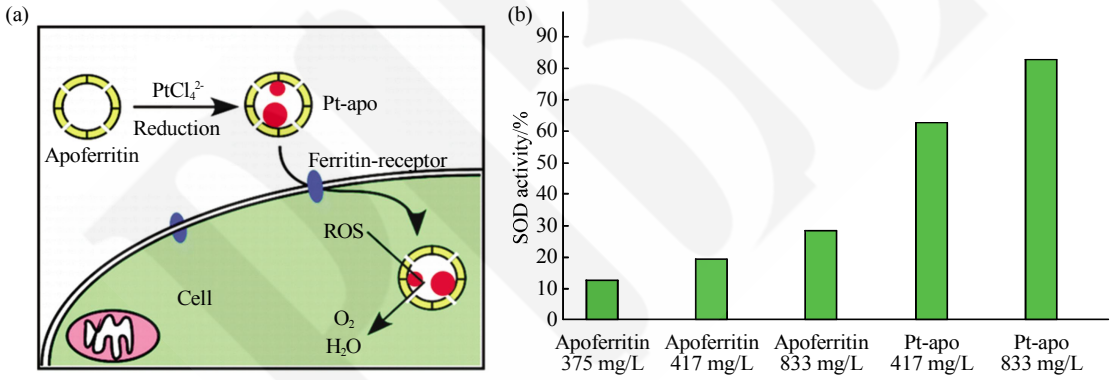

Fig. 10 Pt NPs encapsulated inside apoferritin exhibit enhanced SOD activity

(a) Ferritin-receptor mediates the uptake of this nanoparticle. (b) SOD activity of ferritin and enhanced SOD activity of encapsulated Pt NPs. Reproduced with permission from ref. [77].

to be removed simultaneously for efficient ROS protection[78].

An illustrative example for the use of SOD mimics is to protect cells from ROS in cigarette smoke. ROS of cigarette smoke can damage cells severely. Polyacrylate coated Pt-Np (PAA-Pt) inhibited cell death of alveolar-type Ⅱ A549 cells after cigarette smoke exposure. In an *in vivo* study, intranasal administered PAA-Pt Np also prevented antioxidant depletion, NF-κB activation, and neutrophilic inflammation after three days of cigarette smoke exposure. Interestingly, platinum concentration in their lungs were increased (by 400%), but not in extrapulmonary organs [79]. Further, treatments with platinum NPs and nanocomposites exhibited protective properties in ischemic stroke-, UV light-induced oxidative stress[80-81]. In addition it is encouraging, that Pt NPs are already approved by the Ministry of Health, Labour and Welfare of Japan as additives in consumer products and cosmetics, without reports about serious side effects[79]. Nevertheless, the toxicity of NPs is still not well understood and further research is necessary[82].

3.3 Manganese-containing SOD mimics

In addition to their well-known functions in photosynthesis the divalent forms of Mn are important

in the centers of hydrolytic and phosphate transferring enzymes. Moreover, manganese in higher oxidation states plays a crucial role as redox center in several enzymes like ribonucleotide reductase, catalase, peroxidase and in particular SOD in mitochondria[43, 83-84]. Manganous phosphate was one of the first reported SOD mimics, and MnO_2 is one of the oldest catalyst for the decomposition of H_2O_2. $Mn_3(PO_4)_2$ hollow spheres obtained by a micro-emulsion method detect the release of superoxide anions selectively [85]. Likewise, Mn_3O_4 nanoflowers have SOD, catalase (CAT), and glutathione peroxidase activity (GPx), where the catalytic ability depends on particle size and morphology. Interestingly, Mn_3O_4 nanoparticles with a morphology as flakes, cubes, polyhedron or hexagonal plates lacked GPx and CAT like activity. Except for NP with flake-like morphology SOD activity was reduced by almost 50%～60% (Figure 11). The large pore size of Mn_3O_4 nanoflowers might be responsible for its multienzyme activity, because these pores provide enough space for all substrates or the cofactor GSH [86].

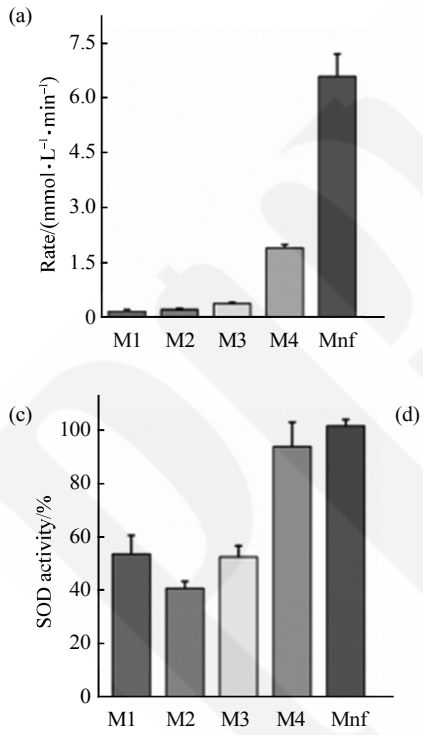

(d)

Code	Size/ (nm)	S_{BET}/ (m^2g^{-1})	V/ (cm^2g^{-1})
M1	50	29.5	0.15
M2	60	28.4	0.18
M3	140	25.7	0.16
M4	100	62.7	0.36
Mnf	180	97.7	0.37

Fig. 11 Morphological dependency of the catalytic ability of Mn_3O_4 NPs

Comparison of (a) CAT, (b) GPx and (c) SOD-like activity of M1 (cubes), M2 (polyhedron), M3 (hexagonal plates), M4 (flakes) with Mnf. (d) Structural parameters of different morphologies of Mn_3O_4 NPs determined by SEM, BET and BJH analyses. Reproduced with permission from ref. [86].

3.3.1 Manganese oxide SOD mimicking nanoparticles enhance MRI contrast

SOD-mimicking MnO NPs, functionalized with a catechol-PEG, were used to improve tumor diagnosis by enhancing their magnetic resonance imaging (MRI) contrast [87]. The approach relies on the fact that the SOD levels in tumor tissue are often reduced while the superoxide radical levels are enhanced. A MRI contrast agent, whose contrast is enhanced by the superoxide concentration, can distinguish between healthy and tumor tissue. When the MnO nanoparticles were exposed to superoxide radicals their relaxation times increased remarkably (compare Figure 12). Different from nanoceria the Mn^{2+}/Mn^{3+} ratio at the NP surface was independent of the SOD-like activity. The MnO NPs are dual enzyme mimics which have SOD and catalase activity simultaneously [87].

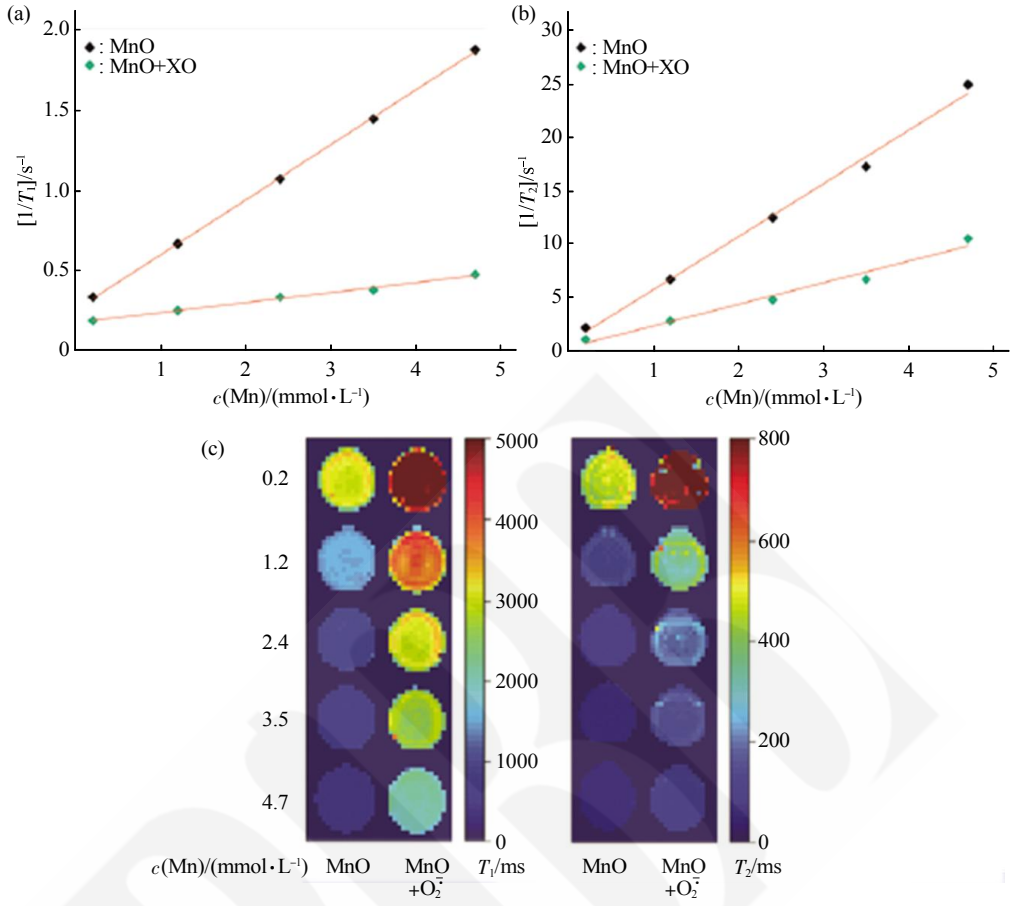

Fig. 12 Manganese oxide SOD mimicking NPs enhance MRI contrast

Specific relaxivities (a) r_1 and (b) r_2 of MnO NPs without and with addition of superoxide generated by XO. Relaxivities were determined by linear regression and show values for MnO NPs without XO of r_1 = (0.35±0.01) mmol^{-1}·L·s^{-1} and r_2 = (4.94±0.11) mmol^{-1}·L·s^{-1}, and for MnO NPs with XO of r_1 = (0.06±0.01) mmol^{-1}·L·s^{-1} and r_2 = (1.90±0.14) mmol^{-1}·L·s^{-1}. (c) MRI imaging of varying MnO concentrations (0.2–4.7 mmol/L) showing T_1-(MnO, left) and T_2-weighted images (MnO, right) with relaxation times (T_1, T_2) measured on a standard clinical MRI instrument using a 96 well-plate with an equilibration time of roughly 60 min. Upon generation of superoxide radicals *in situ* by adding xanthine oxidase, T_1 and T_2 substantially increase, resulting in significant changes in the MRI contrast. Reproduced with permission from ref. [87].

3.3.2 Manganese-containing nanoparticles targeting endothelial cells

A native CuZn-SOD called orgotein attenuates the release of free radicals in the synovial fluid of rheumatoic arthritis patients and showed promising results as a therapeutic in patients with rheumatoid arthritis and osteoarthritis. Although clinical studies in patients with osteoarthritis also revealed amelioration-with respect to signs the drug had to be taken off the market in Germany due to severe allergic reactions and death for several patients [12–13], but the search for alternatives moved on. Mn(Ⅲ) 5, 10, 15, 20-tetrakis (N-methylpyridinium-2-yl)porphyrin (MnTM-4-Pyp) particles, where Mn^{3+} is stabilized by a porphyrin ring, showed an antioxidant /anti-inflammatory effect [88–89]. Metal-centered porphyrins are well known compounds for reversible oxygen binding (*e.g.* in hemoglobin and CuZn-SOD). In combination with tocopherol phosphate MnTM-4-Pyp are among the most potent inhibitors of lipid peroxidation. An important property is to minimize the risk of (Fenton-type) side reactions in pharmaceutical applications. These NPs were conjugated with anti-platelet endothelial cell adhesion molecule (PECAM) antibodies to target endothelial cells [88]. PECAM-1 is a constitutive protein expressed in endothelial cells [88]. *In vitro* studies revealed that treatment with MnTM-4-Pyp reduced the upregulation of vascular cell adhesion molecule 1 (VCAM) in

inflammatory processes. The role of the adhesion protein VCAM and the protection of SOD mimics against proinflammatory endothelial activation is illustrated in Figure 13[88].

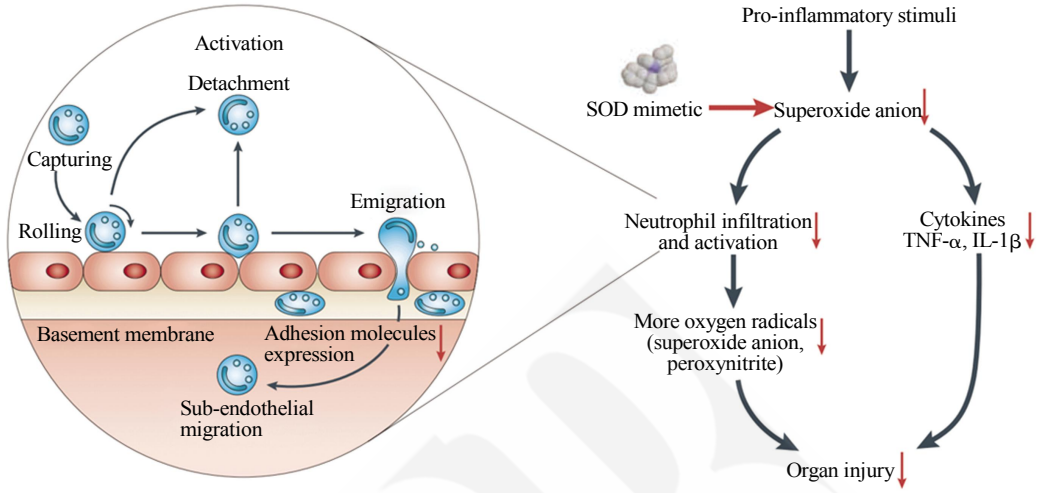

Fig. 13 Proposed scheme of a possible protection mechanism of SOD mimics

In inflammatory cascades, neutrophils and monocytes are migrating sub-endothelially. Adhesion molecules like VCAM1 or ICAM1 proteins facilitate this process. Removal of superoxide anions inhibits the inflammatory cascade through at least three different pathways: less formation of peroxynitrite; inhibition of the migration of different leukocytes migration and inhibition of pro-inflammatory cytokine release. Reproduced with permission from ref. [14].

3.4 Copper-containing SOD mimics

During the reaction cycle, copper shuttles between the oxidations state of Cu(Ⅰ) and Cu(Ⅱ). Although several copper complexes have shown SOD activity *in vitro* [89–91], copper compounds are less promising for pharmaceutical applications because of the toxicity of Cu^{2+} compounds [59]. Moreover, the complexation of Cu^{2+} by a variety of bio-ligands copper *in vivo* decreases the stability of the copper-containing drug [92–94]. Figure 14 shows the appearance of mouse kidneys after oral gavage of copper particles, which is an impressive example to illustrate the toxicity of released free copper ions *in vivo*.

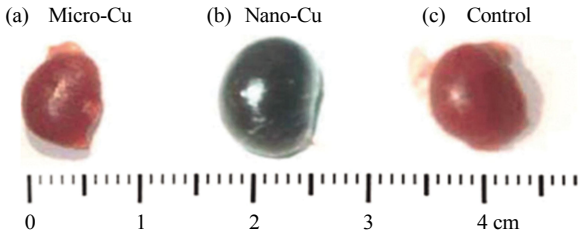

Fig. 14 The appearance of mouse kidneys after oral gavage of copper particles

(a) micro-Cu (1077 mg/kg), (b) nano-Cu (1080 mg/kg) and (c) the control. The toxicity of Cu NPs was comparable to copper salts. Chen *et al*. proposed that the reactivity of Cu NPs is higher because of their high specific surface area. In a reaction with gastric juices toxic copper ions are formed. Reproduced with permission from ref. [92].

Tobacco smoke contains a large number of constituents, including narcotoxic substances such as nicotine, blood toxins like cyanide and carbon monoxide, and various carcinogens. Among them, there are a large amount of ROS, including free oxygen radicals. More than 10 quadrillion (10^{16}) of these molecules are inhaled with every puff on a cigarette. Oxygen derived species such as superoxide radical, hydrogen peroxide, singlet oxygen and hydroxyl radical contained in tobacco smoke are cytotoxic and have been implicated in the etiology of a wide array of human diseases, including lung cancer. The elevated levels of ROS and down regulation of ROS scavengers and antioxidant enzymes are associated with various cancers as well. Therefore, reducing ROS in cigarette smoke is a promising approach for cancer prevention to reduce its prevalence. Recently, Korschelt *et al*. reported a high superoxide scavenging ability of glycine functionalized cuprous hydroxide (Gly-Cu $(OH)_2$) NPs [26], where

copper shuttles between the oxidations state Cu^{+} and Cu^{2+} during the reaction cycle. Remarkably, the Gly-Cu(OH)$_2$) NPs have higher rate constants than the native CuZn-SOD enzyme ($\approx 3.91 \times 10^{10}$ $mol^{-1} \cdot L \cdot s^{-1}$; 1.98×10^{9} $mmol^{-1} \cdot L \cdot s^{-1}$) [26]. Gly-Cu(OH)$_2$ NPs were integrated in cigarette filters and could reduce the levels of free radicals in smoke, hence providing smokers with greater protection against their toxic potential. Cytotoxicity tests showed that the cigarette smoke extracts in the examined concentrations no longer have a toxic effect on human cells after passing through cigarette filters containing nanoparticles, while there was increased toxicity in the case of controls in which untreated filters were employed (Figure 15). It should be noted, however, that detoxification of cigarette smoke with copper compounds has a potential for the formation of polychlorinated dibenzo-p-dioxins and dibenzofurans [95-96]. Another application of copper-based SOD mimics is in electrochemical superoxide sensing[22].

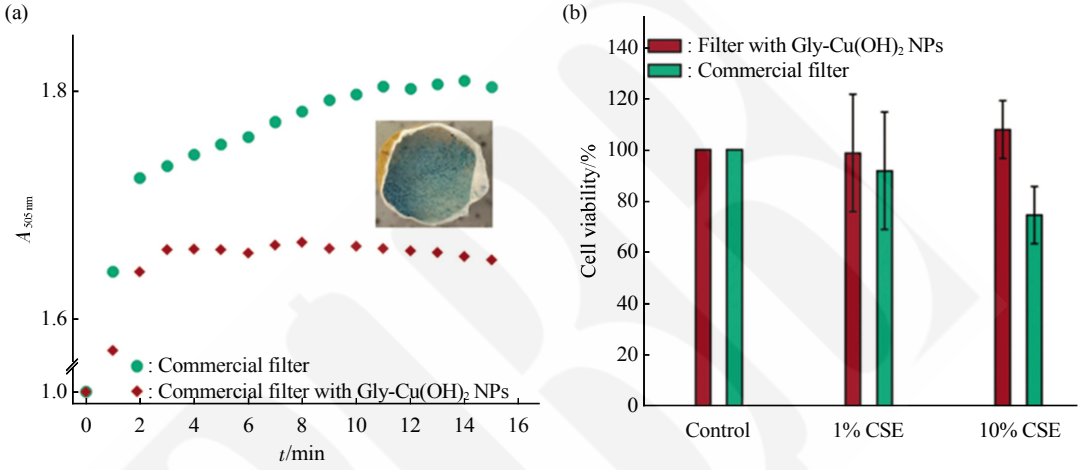

Fig. 15 Catalytic efficiency of Gly-Cu(OH)$_2$ NPs and reduction of superoxide concentration in cigarette smoke

(a) Relative absorption of the reduced INT species at 505 nm for CSE prepared with a commercial filter and a filter containing solid NPs. An inhibition of the INT reduction was observed based on the decomposition of superoxide by Gly-Cu(OH)$_2$ NPs. (b) Cytotoxicity of CSE produced with commercial cigarette filters and with filter systems containing Gly-Cu(OH)$_2$ NPs. Reproduced with permission from ref. [26].

3.5 Cobalt-containing SOD mimics

The SOD activity of Co^{2+} complexes has been reported very early [97]. Dong *et al*. described a pH-dependent Co_3O_4 NP multi-enzyme mimic. In neutral and alkaline solution this NP possesses SOD and catalase activity, while peroxidase-like activity was observed in acidic solution. Co_3O_4 NP were conjugated with antibodies and used in immunohistochemistry for staining sliced tumor tissue [98]. Similarly, $Co_3(PO_4)_2$ NPs were used in electrochemical sensing to detect superoxide anions released from living cells. The detection was selective, *i.e*. there was no significant interferance with ions or molecules like K^{+}, Na^{+}, Cl^{-}, SO_4^{-}, NO_3^{-}, NO or H_2O_2. Moreover, their reported detection limit of 2.25 nmol/L is very low compared many other modified electrodes used in superoxide detection[99]. At this point, we want to compare different developed superoxide anion biosensors based on their detection limit (Table 1).

3.6 Iron-containing SOD mimics

Iron can switch easily between the oxidation states Fe^{2+} and Fe^{3+} and is therefore involved in many enzymatic redox processes [106-107], including those of SOD [43]. Iron oxide NPs have received great attention as enzyme mimics after Yan's discovery of the peroxidase activity of Fe_3O_4 NPs [108], whereas little is known about iron containing NPs with SOD activity. Zhang *et al*. reported the multienzyme-like activity of prussianblue (PB, $[Fe(\text{Ⅲ})Fe(\text{Ⅱ})(CN)_6]^{-}$) NPs, which have SOD, catalase, and peroxidase activity [109]. The mixed valent NPs showed SOD activity over a wide pH range, whereas the catalase activity was enhanced in basic and the peroxidase activity in acidic

Table 1 Comparison of the detection limit of some $O_2^{\cdot-}$ biosensors

(Values were rounded to the third digit)

	Superoxide anion biosensor	Detection limit	Correlation coefficient *R*	Reference
Enzyme and protein based	SOD/Pt-Pd/MWCNTs/SPGE	710 nmol/L	0.997, (R^2= 0.9941)	[100]
	Cytochrome-c based sensor /3-mercaptoethanol monolayer	38 nmol/L		[101]
	nanoporous gold immobilized with cytochrome-c	3.7 nmol/L		[102]
NP-based	$Mn_2P_2O_7$-formylstyrylpyridine/ GCE	29 nmol/L	0.991	[103]
	SiO_2-$Mn^3(PO_4)_2$/MWCNTs/GCE	17.5 nmol/L	0.997	[104]
	$Mn_3(PO_4)_2$/GCE	1.35 nmol/L	0.999	[85]
	DNA-$Mn_3(PO_4)_2$ -carbonnanotubes	3.3 nmol/L	0.999	[105]
	Au-Np+Cu-Cys/CP	250 nmol/L	0.993	[22]
	$Co_3(PO_4)_2$/GCE	2.25 nmol/L	0.999 (R^2= 0.999)	[99]

MWCNTs/SPGE = Multi-walled carbon nanotubes/screen-printed gold film electrodes; GCE = Glassy carbon electrode; Gold nanoparticles = Au-Np; copper(Ⅱ) complex of cysteine = Cu-Cys; carbon paste electrode = CP

conditions. The ROS scavenging ability of the PB NPs was demonstrated with a series of *in vitro* ROS-generating models using chemicals, UV irradiation, oxidized low-density lipoprotein, high glucose contents, and oxygen glucose deprivation and reperfusion. An *in vivo* inflammation model was established using lipoproteins in mice. The PB NPs could relieve injury induced by ROS in these pathological processes. Besides Prussian blue nanoparticles, also iron phosphate microflowers exhibited SOD and peroxidase like activity [110].

3.7 Carbon-based SOD mimics—fullerenes

C_{60} fullerenes were the first established nanozymes [16]. After their discovery in 1985 by Kroto *et al*., Krusic *et al*. found that C_{60} fullerene exhibits radical scavenging properties like a radial sponge [111]. Encouraged by these findings, water soluble fullerene derivatives were explored for pharmaceutical applications [112]. Fullerenols, hexasulfobutyl fullerenes, or carboxy fullerenes are the most popular examples [112]. A first major break-through for fullerenes as SOD mimcs was the application of tris-malonyl-C_{60} derivates [112]. After Dugan *et al*. reported neuroprotective properties of buckministerfullerenols [113], Sameh *et al*. showed that the C_3 regioisomer of tris-malonyl-C_{60} exhibit SOD activity rather than being a stochiometric radical scavenger [114]. Their proposed reaction mechanism is shown in Figure 16. Although the fullerene SOD mimic shows 100 times less catalytic activity (2×10^6 mol•s^{-1}) than that of native enzymes or other NPs with SOD activity [114], they were tested for different treatments. C_{60}-C_3 fullerene could prolong the lifetime of SOD (Mn-SOD) knockout mice by approximately 300% after daily injection [114]. As fullerene chemistry is a very broad topic, we cannot give a comprehensive overview. Possible benefits of fullerene derivates in neurodegenerative diseases have been shown by Dugan *et al*. [23, 113]. Polyhydroxylated fullerenes reduced excitotoxicity and apoptosis of cortical neurons of mice induced by NMDA, AMPA, or kainite (measured as lactate dehydrogenase release). Their neuroprotective effects were confirmed by many other groups in *in vitro* and in *in vivo* models [23, 115–117]. Quick *et al*. showed the ability of the C_3 regioisomer of tris-malonic acid C_{60} fullerene derivative to reduce oxidative stress caused by aging in brains of wild-type mice [117].

Different from other SOD mimics, C_{60} fullerenes are not only SOD mimics. They also have the unique ability to inhibit β-sheet formation [118–120] which has been a major strategy in the treatment of neurodegenerative diseases as Alzheimer. C_{60} derivatives prevent hydrophobic and aromatic stacking interactions of Aβ(16–22) peptides. These interactions are important for β-sheet formation of Aβ-peptides [119]. Besides their neuroprotective effects the protective properties in drugs and xenobiotic ROS damage were studied. Halenova *et al*. studied the hepatoprotective effect of pristine C_{60} fullerene. As a model of xenobiotic-induced hepatotoxicity, liver injury was induced by injecting CCl_4, damaging effects are caused by free radical formation in liver cells. After toxification, pro-inflammatory cytokine levels increased by 25%–50%, while 1.5 g/L previous orally

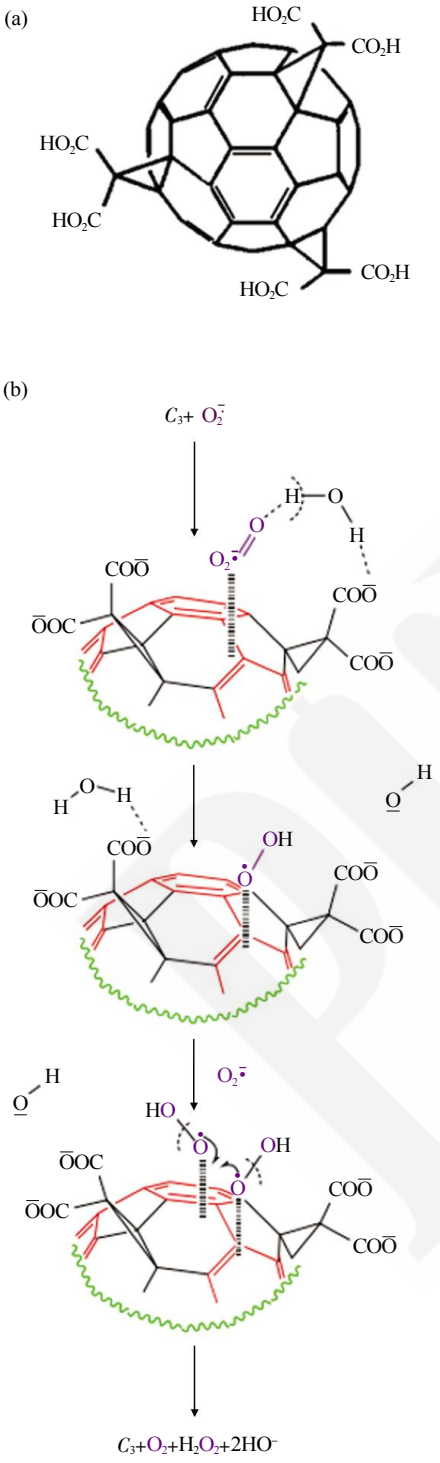

Fig. 16 Molecular stucture and reaction mechanism of a tris-malonyl-C_{60} derivate catalyzing the disproportionation

(a) Molecular structure. (b) The proposed reaction cycle of C_3 regioisomer of tris-malonic acid C_{60} catalyzing the disproportionation of superoxide. Reproduced with permission from ref. [114].

administered water-soluble C_{60} fullerenes kept the liver cytokine levels normal. Since the toxicity of doxorubicin is caused mainly by the generation of oxidative stress, fullerenes combined with doxorubicin is considered a potential synergetic cancer treatment[121]. In cosmetics, fullerenes have been used as radical scavengers, examples are shown in Figure 17[122].

Zelens® fullerene C_{60} night cream

Radical sponge® - Vitamin C_{60} BioResearch corporation

LipoFullerene® - Vitamin C_{60} BioResearch corporation

Fig. 17 Commercially available products containing fullerenes

Reproduced with permission from ref. [122].

Enzyme mimics can also be used in many different research areas and applications apart from medicine. For instance, Czochara *et al*. have shown that fullerene C_{60}, conjugated with phenols, are hybrid antioxidants that can increase the oxidative stability of polymers at higher temperatures [25]. The radical scavenging properties of C_{60} combined with its stability up to 600℃ make it a good candidate. The oxidation rate of high density polyethylene with polyethylene containing 5% 2, 6-di-*tert*-butyl-4-methylphenol (BHT), a widely used antioxidant in polymers was investigated. All tested fullerene derivates exhibited higher stabilizing effects. Furthermore, the temperature where oxidation starts was increased by 30–40 degrees when fullerene additives were added. Fullerene have numerous of useful properties in photovoltaics, as photocatalysts or fuel cells[122].

4 Conclusion

Oxidative stress is a normal physiological phenomenon, where the intracellular ROS levels are maintained by several enzyme systems, among them SODs, participating in the *in vivo* redox homeostasis. In essence, oxidative stress can be viewed as an imbalance between the pro- and anti-oxidants in the cells and organism.

Clinical use of the native or recombinant SODs is hampered by the factors such as instability, limited cellular accessibility, immunogenicity, short half-life, and high production costs. Due to these limitations, SOD mimetics have been proposed for the application under degenerative pathological conditions.

This review introduces some basic ideas of enzyme evolution and heterogenous catalysis to improve our understanding of the mechanism of NPs with SOD-like activity. It highlights different nanoparticle-based SOD mimics (nanozymes), which can overcome some challenges of native or recombinant SODs and gives a broad overview for treatment strategies with SOD nanozymes. Applications apart from pharmaceutical treatments like the ROS reduction in cigarette smoke or as antioxidative additives in polymers are lucid examples of abundant SOD uses. A short summary of different nanozymes and their apllications is shown in Table 2. Although the results are encouraging, a detailed toxicologic assessments of different NPs is still necessary and will be essential for further breakthrough of nanozymes in medicine.

Table 2 SOD nanozymes and their applications

Nanomaterial	Activity	Application	Reference
CeO_2	SOD, CAT	Cell protection in radiation therapy	[123]
		Anti-inflammation	[21]
		Neuroprotection	[18, 20, 65, 70]
		Anticancer-treatment	[124]
		Wound healing	[125]
Apoferritin-encapsulated Pt NP	SOD, CAT	Protection against oxidative stress	[77]
Pt NP	SOD, CAT	Neuro-protection	[81]
		Pulmonary inflammation	[79]
Au-Pt NP	SOD, CAT	Scavenging UV-induced cellular ROS	[80]
SiO_2-$Mn_3(PO_4)_2$ and $Mn_3(PO_4)_2$ hollow spheres	SOD	Electrochemical detection of superoxide anions	[104, 85]
Mn_3O_4 nanoflowers	SOD, CAT, GPx	Cyto-protection in Parkinson disease	[126]
MnO	SOD, CAT	Nanoparticle to enhance the magnetic resonance imaging contrast	[87]
Gly-$Cu(OH)_2$ NPs	SOD	Reducing ROS in cigarette smoke	[26]
$FePO_4$ microflowers	POD, SOD		[110]
$[Fe(Ⅲ)Fe(Ⅱ)(CN)]_6^-$	POD, CAT, SOD	Protection against oxidative stress	[109]
Co_3O_4	POD, SOD, CAT	Immunohistochemistry detection	[98]
C_{60} fullerene derivates	SOD	Protection against xenobiotic-induced oxidative stress	[121, 127]
		Neuroprotection	[23, 113, 118−119, 128]
		Improving the oxidative stability of polymers at elevated temperatures	[25]

References

[1] Yang Y, Bazhin A V, Werner J, *et al*. Reactive oxygen species in the immune system. Int Rev Immunol, 2013, **32**(3): 249−270

[2] Karakoti A, Singh S, Dowding J M, *et al*. Redox-active radical scavenging nanomaterials. Chem Soc Rev, 2010, **39**(11): 4422−4432

[3] Das S K, Vasudevan D M. Alcohol-induced oxidative stress. Life Sci, 2007, **81**(3): 177−187

[4] Valavanidis A, Vlachogianni T, Fiotakis K. Tobacco smoke: Involvement of reactive oxygen species and stable free radicals in mechanisms of oxidative damage, carcinogenesis and synergistic effects with other respirable particles. Int J Env Res Pub He, 2009, **6**(2): 445−462

[5] Hanson K M, Gratton E, Bardeen C J. Sunscreen enhancement of UV-induced reactive oxygen species in the skin. Free Radical Bio Med, 2006, **41**(8): 1205−1212

[6] Prasad S, Gupta S C, Tyagi A K. Reactive oxygen species (ROS) and cancer: Role of antioxidative nutraceuticals. Cancer Lett, 2017, **387**(2): 95−105

[7] McCord J M. Human disease, free radicals, and the oxidant/antioxidant balance. Clin Biochem, 1993, **26**(5): 351−357

[8] Jenner P. Oxidative stress in Parkinson's disease. Ann Neurol, 2003, **53**(3): 26−38

[9] Madamanchi N R, Vendrov A, Runge M S. Oxidative stress and

vascular disease. Arterioscler Thromb Vasc Biol, 2005, **25** (1): 29-38

[10] Praticò D, Basili S, Vieri M, *et al*. Chronic obstructive pulmonary disease is associated with an increase in urinary levels of isoprostane F2alpha-Ⅲ, an index of oxidant stress. Am J Resp Crit Care, 1998, **158**(6): 1709-1714

[11] Kaneto H, Katakami N, Matsuhisa M, *et al*. Role of reactive oxygen species in the progression of type 2 diabetes and atherosclerosis. Mediat Inflamm, 2010, **2010**: 1-11

[12] GOEBEL K, Storck U, Neurath, *et al*. Intrasynovial orgotein therapy in rheumatoid arthritis. Lancet, 1981, **317** (8228): 1015-1017

[13] Arzneimittelkommission der deutschen Ärzteschaft. orgotein-haltige Arzneimittel. Deutsches Ärzteblatt, 1994, **91**(8): A-517

[14] Salvemini D, Riley D P, Cuzzocrea S. SOD mimetics are coming of age. Nat Rev Drug Discov, 2002, **1**(5): 367-374

[15] Cleaves H J, Michalkova Scott A, Hill F C, *et al*. Mineral-organic interfacial processes: Potential roles in the origins of life. Chem Soc Rev, 2012, **41**(16): 5502-5525

[16] Wei H, Wang E. Nanomaterials with enzyme-like characteristics (nanozymes): Next-generation artificial enzymes. Chem Soc Rev, 2013, **42**(14): 6060-6093

[17] Shilo M, Sharon A, Baranes K, *et al*. The effect of nanoparticle size on the probability to cross the blood-brain barrier: An *in vitro* endothelial cell model. J Nanobiotechnol, 2015, **13**(1): 19

[18] Heckman K L, DeCoteau W, Estevez A, *et al*. Custom cerium oxide nanoparticles protect against a free radical mediated autoimmune degenerative disease in the brain. ACS Nano, 2013, **7** (12): 10582-10596

[19] Chen J, Patil S, Seal S, *et al*. Rare earth nanoparticles prevent retinal degeneration induced by intracellular peroxides. Nat Nanotechnol, 2006, **1**(2): 142-150

[20] Kim C K, Kim T, Choi I Y, *et al*. Ceria nanoparticles that can protect against ischemic stroke. Angew Chem Int Edit, 2012, **51**(44): 11039-11043

[21] Hirst S M, Karakoti A S, Tyler R D, *et al*. Anti-inflammatory properties of cerium oxide nanoparticles. Small, 2009, **5** (24): 2848-2856

[22] Dashtestani F, Ghourchian H, Eskandari K, *et al*. A superoxide dismutase mimic nanocomposite for amperometric sensing of superoxide anions. Microchim Acta, 2015, **182**(5-6): 1045-1053

[23] Dugan L L, Turetsky D M, Du C, *et al*. Carboxyfullerenes as neuroprotective agents. Proc Natl Acad Sci USA, 1997, **94** (17): 9434-9439

[24] Das S, Dowding J M, Klump K E, *et al*. Cerium oxide nanoparticles: Applications and prospects in nanomedicine. Nanomedicine, 2013, **8**(9): 1483-1508

[25] Czochara R, Kusio J, Litwinienko G. Fullerene C_{60} conjugated with phenols as new hybrid antioxidants to improve the oxidative stability of polymers at elevated temperatures. RSC Adv, 2017, **7**(70): 44021-44025

[26] Korschelt K, Ragg R, Metzger C S, *et al*. Glycine-functionalized copper(Ⅱ) hydroxide nanoparticles with high intrinsic superoxide dismutase activity. Nanoscale, 2017, **9**(11): 3952-3960

[27] Colín-García M, Heredia A, Cordero G, *et al*. Hydrothermal vents and prebiotic chemistry: a review. B Soc Geol Mex, 2016, **68**(3): 599-620

[28] Bachmann B O. Biosynthesis: Is it time to go retro? Nat Chem Biol, 2010, **6**(6): 390-393

[29] Horowitz N H. On the evolution of biochemical syntheses. Proc Natl Acad Sci USA, 1945, **31**(6): 153-157

[30] Zuckerkandl E. The appearance of new structures and functions in proteins during evolution. J Mol Evol, 1975, **7**(1): 1-57

[31] Li Y, He X, Yin J J, *et al*. Acquired superoxide-scavenging ability of ceria nanoparticles. Angew Chem Int Edit, 2015, **54** (6): 1832-1835

[32] Celardo I, Pedersen J Z, Traversa E, *et al*. Pharmacological potential of cerium oxide nanoparticles. Nanoscale, 2011, **3** (4): 1411-1420

[33] Asati A, Santra S, Kaittanis C, *et al*. Oxidase-like activity of polymer-coated cerium oxide nanoparticles. Angew Chem, 2009, **121**(13): 2344-2348

[34] Kuchma M H, Komanski C B, Colon J, *et al*. Phosphate ester hydrolysis of biologically relevant molecules by cerium oxide nanoparticles. Nanomed-Nanotechnol, 2010, **6**(6): 738-744

[35] Jiao X, Song H, Zhao H, *et al*. Well-redispersed ceria nanoparticles: Promising peroxidase mimetics for H_2O_2 and glucose detection. Anal Methods-UK, 2012, **4**(10): 3261-3267

[36] Martin W, Baross J, Kelley D, *et al*. Hydrothermal vents and the origin of life. Nat Rev Microbiol, 2008, **6**(11): 805-814

[37] Hansard S P, Easter H D, Voelker B M. Rapid reaction of nanomolar Mn(Ⅱ) with superoxide radical in seawater and simulated freshwater. Environ Sci Technol, 2011, **45** (7): 2811-2817

[38] Barnese K, Gralla E B, Valentine J S, *et al*. Biologically relevant mechanism for catalytic superoxide removal by simple manganese compounds. Proc Natl Acad Sci USA, 2012, **109**(18): 6892-6897

[39] Barnese K, Gralla E B, Cabelli D E, *et al*. Manganous phosphate acts as a superoxide dismutase. J Am Chem Soc, 2008, **130** (14): 4604-4606

[40] Archibald F S, Fridovich I. Manganese, superoxide dismutase, and oxygen tolerance in some lactic acid bacteria. J Bacteriol, 1981, **146**(3): 928-936

[41] Sheng Y, Butler Gralla E, Schumacher M, *et al*. Six-coordinate manganese (3+) in catalysis by yeast manganese superoxide dismutase. Proc Natl Acad Sci USA, 2012, **109**(36): 14314-14319

[42] Miller A-F. Superoxide dismutases: Ancient enzymes and new insights. FEBS Lett, 2012, **586**(5): 585-595

[43] Sheng Y, Abreu I A, Cabelli D E, *et al*. Superoxide dismutases and superoxide reductases. Chem Rev, 2014, **114**(7): 3854-3918

[44] Yikilmaz E, Rodgers D W, Miller A F. The crucial importance of chemistry in the structure-function link: Manipulating hydrogen bonding in iron-containing superoxide dismutase. Biochemistry-US, 2006, **45**(4): 1151-1161

[45] Koppenol W H, Levine F, Hatmaker T L, *et al*. Catalysis of superoxide dismutation by manganese aminopolycarboxylate complexes. Arch Biochem Biophys, 1986, **251**(2): 594-599

[46] Sanchez R J, Srinivasan C, Munroe W H, *et al*. Exogenous manganous ion at millimolar levels rescues all known dioxygen-sensitive phenotypes of yeast lacking CuZnSOD. J Biol Inorg Chem, 2005, **10**(8): 913-923

[47] Kozlov Y N, Zharmukhamedov S K, Tikhonov K G, *et al*. Oxidation potentials and electron donation to photosystem Ⅱ of manganese complexes containing bicarbonate and carboxylate

ligands. Phys Chem Chem Phys, 2004, **6**(20): 4905−4911

[48] David R. Lide. CRC handbook of chemistry and physics: A ready-reference book of chemical and physical data. 85th ed. Boca Raton: CRC Press, Internet Version 2005, <http://wwwhbcpnetbasecom>

[49] Pierre J L, Fontecave M. Iron and activated oxygen species in biology: The basic chemistry. BioMetals, 1999, **12**(3): 195−199

[50] Rizvi M A. Complexation modulated redox behavior of transition metal systems (review). Russ J Gen Chem, 2015, **85**(4): 959−973

[51] Tovmasyan A, Sheng H, Weitner T, *et al*. Design, mechanism of action, bioavailability and therapeutic effects of mn porphyrin-based redox modulators. Med Prin Pract, 2013, **22**(2): 103−130

[52] Deutschmann O, Knözinger H, Kochloefl K, *et al*. Heterogeneous catalysis and solid catalysts//Ullmann's Encyclopedia of Industrial Chemistry. Wiley-VCH Verlag GmbH & Co. KGaA, 2009

[53] Hoffmann R. A chemical and theoretical way to look at bonding on surfaces. Rev Mod Phys, 1988, **60**(3): 601−628

[54] Peter M, Flores Camacho J M, Adamovski S, *et al*. Trends in the binding strength of surface species on nanoparticles: How does the adsorption energy scale with the particle size? Angew Chem Int Edit, 2013, **52**(19): 5175−5179

[55] Medford A J, Vojvodic A, Hummelshøj J S, *et al*. From the Sabatier principle to a predictive theory of transition-metal heterogeneous catalysis. J Catal, 2015, **328**: 36−42

[56] Shao M, Peles A, Shoemaker K. Electrocatalysis on platinum nanoparticles: Particle size effect on oxygen reduction reaction activity. Nano Lett, 2011, **11**(9): 3714−3719

[57] Sun C, Li H, Chen L. Nanostructured ceria-based materials: Synthesis, properties, and applications. Energ Environ Sci, 2012, **5**(9): 8475−8505

[58] Korsvik C, Patil S, Seal S, *et al*. Superoxide dismutase mimetic properties exhibited by vacancy engineered ceria nanoparticles. Chem Commun, 2007(10): 1056−1058

[59] Lanone S, Rogerieux F, Geys J, *et al*. Comparative toxicity of 24 manufactured nanoparticles in human alveolar epithelial and macrophage cell lines. Part Fibre Toxicol, 2009, **6**: 14

[60] Deshpande S, Patil S, Kuchibhatla S V, *et al*. Size dependency variation in lattice parameter and valency states in nanocrystalline cerium oxide. Appl Phys Lett, 2005, **87**(13): 133113

[61] Montini T, Melchionna M, Monai M, *et al*. Fundamentals and catalytic applications of CeO_2-based materials. Chem Rev, 2016, **116**(10): 5987−6041

[62] Pirmohamed T, Dowding J M, Singh S, *et al*. Nanoceria exhibit redox state-dependent catalase mimetic activity. Chem Commun, 2010, **46**(16): 2736−2738

[63] Torbrügge S, Reichling M, Ishiyama A, *et al*. Evidence of subsurface oxygen vacancy ordering on reduced CeO_2(111). Phys Rev Lett, 2007, **99**(5): 56101

[64] Roger V L, Go A S, Lloyd-Jones D M, *et al*. Heart disease and stroke statistics--2012 update: A report from the American Heart Association. Circulation, 2012, **125**(1): e2-e220

[65] Kwon H J, Cha M Y, Kim D, *et al*. Mitochondria-targeting ceria nanoparticles as antioxidants for Alzheimer's Disease. ACS Nano, 2016, **10**(2): 2860−2870

[66] Dowding J M, Song W, Bossy K, *et al*. Cerium oxide nanoparticles protect against Aβ -induced mitochondrial fragmentation and neuronal cell death. Cell Death Differ, 2014, **21**(10): 1622−1632

[67] Gao N, Dong K, Zhao A, *et al*. Polyoxometalate-based nanozyme: Design of a multifunctional enzyme for multi-faceted treatment of Alzheimer's disease. Nano Res, 2016, **9**(4): 1079−1090

[68] Guan Y, Li M, Dong K, *et al*. Ceria/POMs hybrid nanoparticles as a mimicking metallopeptidase for treatment of neurotoxicity of amyloid-β peptide. Biomaterials, 2016, **98**: 92−102

[69] Li M, Shi P, Xu C, *et al*. Cerium oxide caged metal chelator: Anti-aggregation and anti-oxidation integrated H_2O_2-responsive controlled drug release for potential Alzheimer's disease treatment. Chem Sci, 2013, **4**(6): 2536−2542

[70] Estevez A Y, Pritchard S, Harper K, *et al*. Neuroprotective mechanisms of cerium oxide nanoparticles in a mouse hippocampal brain slice model of ischemia. Free Radical Bio Med, 2011, **51**(6): 1155−1163

[71] Ferri C P, Prince M, Brayne C, *et al*. Global prevalence of dementia: A Delphi consensus study. Lancet, 2005, **366**(9503): 2112−2117

[72] Prince M, Wimo A, Guerchet M, *et al*. world Alzheimer report 2015: The global impact of dementia an analysis of prevalence, encidence, cost and trends. Alzheimer's Disease International, 2015

[73] Hamley I W. The amyloid beta peptide: A chemist's perspective. Role in Alzheimer's and fibrillization. Chem Rev, 2012, **112**(10): 5147−5192

[74] Kajita M, Hikosaka K, Iitsuka M, *et al*. Platinum nanoparticle is a useful scavenger of superoxide anion and hydrogen peroxide. Free Radic Res, 2007, **41**(6): 615−626

[75] Kim J, Takahashi M, Shimizu T, *et al*. Effects of a potent antioxidant, platinum nanoparticle, on the lifespan of Caenorhabditis elegans. Mech Ageing Dev, 2008, **129**(6): 322−331

[76] Shen X, Liu W, Gao X, *et al*. Mechanisms of oxidase and superoxide dismutation-like activities of gold, silver, platinum, and palladium, and their alloys: A general way to the activation of molecular oxygen. J Am Chem Soc, 2015, **137**(50): 15882−15891

[77] Zhang L, Laug L, Münchgesang W, *et al*. Reducing stress on cells with apoferritin-encapsulated platinum nanoparticles. Nano Lett, 2010, **10**(1): 219−223

[78] Bafana A, Dutt S, Kumar S, *et al*. Superoxide dismutase: An industrial perspective. Crit Rev Biotechnol, 2011, **31**(1): 65−76

[79] Onizawa S, Aoshiba K, Kajita M, *et al*. Platinum nanoparticle antioxidants inhibit pulmonary inflammation in mice exposed to cigarette smoke. Pulm Pharmacol Ther, 2009, **22**(4): 340−349

[80] Xiong B, Xu R, Zhou R, *et al*. Preventing UV induced cell damage by scavenging reactive oxygen species with enzyme-mimic Au-Pt nanocomposites. Talanta, 2014, **120**: 262−267

[81] Takamiya M, Miyamoto Y, Yamashita T, *et al*. Strong neuroprotection with a novel platinum nanoparticle against ischemic stroke- and tissue plasminogen activator-related brain damages in mice. Neuroscience, 2012, **221**: 47−55

[82] Pedone D, Moglianetti M, Luca E de, *et al*. Platinum nanoparticles in nanobiomedicine. Chem Soc Rev, 2017, **46**(16): 4951−4975

[83] Dismukes G C. Manganese enzymes with binuclear active sites. Chem Rev, 1996, **96**(7): 2909−2926

[84] Terrak M, Kerff F, Langsetmo K, *et al*. Structural basis of protein phosphatase 1 regulation. Nature, 2004, **429**(6993): 780−784

[85] Wang M Q, Ye C, Bao S-J, *et al*. Controlled synthesis of $Mn_3(PO_4)_2$ hollow spheres as biomimetic enzymes for selective detection of

superoxide anions released by living cells. Microchim Acta, 2017, **184**(4): 1177-1184

[86] Mugesh G, Singh N, Savanur M A, *et al*. Redox modulatory Mn_3O_4 nanozyme with multi-enzyme activity provides efficient cytoprotection to human cells in Parkinson's disease model. Angew Chem Int Edit, 2017: 14455-14459

[87] Ragg R, Schilmann A M, Korschelt K, *et al*. Intrinsic superoxide dismutase activity of MnO nanoparticles enhances the magnetic resonance imaging contrast. J Mater Chem B, 2016, **4** (46): 7423-7428

[88] Howard M D, Hood E D, Greineder C F, *et al*. Targeting to endothelial cells augments the protective effect of novel dual bioactive antioxidant/anti-inflammatory nanoparticles. Mol Pharm, 2014, **11**(7): 2262-2270

[89] Khalid H, Hanif M, Hashmi M, *et al*. Copper complexes of bioactive ligands with superoxide dismutase activity. MRMC, 2013, **13**(13): 1944-1956

[90] Tabbì G, Driessen W L, Reedijk J, *et al*. High superoxide dismutase activity of a novel, intramolecularly imidazolato-bridged asymmetric dicopper(Ⅱ) species. design, synthesis, structure, and magnetism of copper(Ⅱ) complexes with a mixed pyrazole imidazole donor set. Inorg Chem, 1997, **36**(6): 1168-1175

[91] Czapski G, Goldstein S. The uniqueness of superoxide dismutase (SOD) — why cannot most copper compounds substitute sod *in vivo*? Free Radical Res Com, 2009, **4**(4): 225-229

[92] Chen Z, Meng H, Xing G, *et al*. Acute toxicological effects of copper nanoparticles *in vivo*. Toxicol Lett, 2006, **163**(2): 109-120

[93] Midander K, Cronholm P, Karlsson H L, *et al*. Surface characteristics, copper release, and toxicity of nano- and micrometer-sized copper and copper(Ⅱ) oxide particles: A cross-disciplinary study. Small, 2009, **5**(3): 389-399

[94] Karlsson H L, Cronholm P, Gustafsson J, *et al*. Copper oxide nanoparticles are highly toxic: A comparison between metal oxide nanoparticles and carbon nanotubes. Chem Res Toxicol, 2008, **21**(9): 1726-1732

[95] Lenoir D, Schramm K W. Comment on "Glycine-functionalized copper (ii) hydroxide nanoparticles with high intrinsic superoxide dismutase activity" by K. Korschelt, R. Ragg, C. S. Metzger, M. Kluenker, M. Oster, B. Barton, M. Panthöfer, D. Strand, U. Kolb, M. Mondeshki, S. Strand, J. Brieger, M. N. Tahir and W. Tremel, Nanoscale, 2017, **9**, 3952. Nanoscale, 2017, **9**(40): 15717-15718

[96] Dickson L C, Lenoir D, Hutzinger O. Quantitative comparison of *de novo* and precursor formation of polychlorinated dibenzo-p-dioxins under simulated municipal solid waste incinerator postcombustion conditions. Environ Sci Technol, 1992, **26**(9): 1822-1828

[97] Anacona J R, Azocar M, Nusetti O, *et al*. Crystal structure of the first SH-containing tetrahedral cobalt(Ⅱ) complex, $[Co(quinoline)_2(SH)_2]$. Superoxide dismutase activity. Transit Metal Chem, 2003, **28**(1): 24-28

[98] Dong J, Song L, Yin J J, *et al*. Co_3O_4 nanoparticles with multi-enzyme activities and their application in immunohistochemical assay. ACS Appl Mater Inter, 2014, **6**(3): 1959-1970

[99] Wang M Q, Ye C, Bao S J, *et al*. Nanostructured cobalt phosphates as excellent biomimetic enzymes to sensitively detect superoxide anions released from living cells. Biosens Bioelectron, 2017, **87**: 998-1004

[100]Zhu X, Niu X, Zhao H, *et al*. Immobilization of superoxide dismutase on Pt-Pd/MWCNTs hybrid modified electrode surface for superoxide anion detection. Biosens Bioelectron, 2015, **67**: 79-85

[101]Chen X J, West A C, Cropek D M, *et al*. Detection of the superoxide radical anion using various alkanethiol monolayers and immobilized cytochrome c. Anal Chem, 2008, **80**(24): 9622-9629

[102]Sadeghian R B, Ostrovidov S, Han J, *et al*. Online monitoring of superoxide anions released from skeletal muscle cells using an electrochemical biosensor based on thick-film nanoporous gold. ACS Sensors, 2016, **1**(7): 921-928

[103]Yuan L, Liu S, Tu W, *et al*. Biomimetic superoxide dismutase stabilized by photopolymerization for superoxide anions biosensing and cell monitoring. Anal Chem, 2014, **86**(10): 4783-4790

[104]Shen X, Wang Q, Liu Y, *et al*. Manganese phosphate self-assembled nanoparticle surface and its application for superoxide anion detection. Sci Rep, 2016, **6**: 28989

[105]Ma X, Hu W, Guo C, *et al*. DNA-templated biomimetic enzyme sheets on carbon nanotubes to sensitively *in situ* detect superoxide anions released from cells. Adv Funct Mater, 2014, **24** (37): 5897-5903

[106]Yates M G, Nason A. Electron transport system of the chemoautotroph ferrobacillus ferrooxidans. J Biol Chem, 1966, **241**(21): 4872-4880

[107]Visser SP de, Kumar D. Iron-containing enzymes: versatile catalysts of hydroxylation reactions in nature; [non-heme versus heme]. Cambridge: Royal Society of Chemistry, 2011

[108]Gao L, Zhuang J, Nie L, *et al*. Intrinsic peroxidase-like activity of ferromagnetic nanoparticles. Nat Nanotechnol, 2007, **2** (9): 577-583

[109]Zhang W, Hu S, Yin J J, *et al*. Prussian blue nanoparticles as multienzyme mimetics and reactive oxygen species scavengers. J Am Chem Soc, 2016, **138**(18): 5860-5865

[110]Wang W, Jiang X, Chen K. Iron phosphate microflowers as peroxidase mimic and superoxide dismutase mimic for biocatalysis and biosensing. Chem Commun, 2012, **48**(58): 7289-7291

[111]Krusic P J, Wasserman E, Keizer P N, *et al*. Radical reactions of C60. Science, 1991, **254**(5035): 1183-1185

[112]Cataldo F, Milani P, Ros T. Medicinal chemistry and pharmacological potential of fullerenes and carbon nanotubes: medicinal chemistry and pharmacological potential of fullerenes and carbon nanotubes. 1st ed. sl: Springer Netherlands, 2008

[113]Dugan L L, Gabrielsen J K, Yu S P, *et al*. Buckminsterfullerenol free radical scavengers reduce excitotoxic and apoptotic death of cultured cortical neurons. Neurobiol Dis, 1996, **3**(2): 129-135

[114]Ali S S, Hardt J I, Quick K L, *et al*. A biologically effective fullerene (C_{60}) derivative with superoxide dismutase mimetic properties. Free Radical Bio Med, 2004, **37**(8): 1191-1202

[115]Vorobyov V, Kaptsov V, Gordon R, *et al*. Neuroprotective effects of hydrated fullerene C_{60}: Cortical and hippocampal EEG interplay in an amyloid-infused rat model of Alzheimer's disease. J Alzheimers Dis, 2015, **45**(1): 217-233

[116]Dugan L L, Lovett E G, Quick K L, *et al*. Fullerene-based antioxidants and neurodegenerative disorders. Parkinsonism Relat D, 2001, **7**(3): 243-246

[117]Quick K L, Ali S S, Arch R, *et al*. A carboxyfullerene SOD mimetic improves cognition and extends the lifespan of mice. Neurobiol Aging, 2008, **29**(1): 117-128

[118]Kim J E, Lee M. Fullerene inhibits β-amyloid peptide aggregation. Biochem Bioph Res Co, 2003, **303**(2): 576−579

[119]Xie L, Luo Y, Lin D, *et al*. The molecular mechanism of fullerene-inhibited aggregation of Alzheimer's β -amyloid peptide fragment. Nanoscale, 2014, **6**(16): 9752−9762

[120]Lei J, Qi R, Xie L, *et al*. Inhibitory effect of hydrophobic fullerenes on the β-sheet-rich oligomers of a hydrophilic GNNQQNY peptide revealed by atomistic simulations. RSC Adv, 2017, **7** (23): 13947−13956

[121]Prylutska S, Grynyuk I, Matyshevska O, *et al*. C_{60} fullerene as synergistic agent in tumor-inhibitory Doxorubicin treatment. Drugs R&D, 2014, **14**(4): 333−340

[122]Acquah S F A, Penkova A V, Markelov D A, *et al*. Review——the beautiful molecule: 30 years of C_{60} and its derivatives. ECS J Solid State Sc, 2017, **6**(6): M3155-M3162

[123]Tarnuzzer R W, Colon J, Patil S, *et al*. Vacancy engineered ceria nanostructures for protection from radiation-induced cellular damage. Nano Lett, 2005, **5**(12): 2573−2577

[124]Giri S, Karakoti A, Graham R P, *et al*. Nanoceria: A rare-earth nanoparticle as a novel anti-angiogenic therapeutic agent in ovarian cancer. Plos One, 2013, **8**(1): e54578

[125]Davan R, Prasad RGSV, Jakka V S, *et al*. Cerium oxide nanoparticles promotes wound healing activity in *in vivo* animal model. J Bionanosci, 2012, **6**(2): 78−83

[126]Mugesh G, Singh N, Savanur M A, *et al*. Redox modulatory Mn_3O_4 nanozyme with multi-enzyme activity provides efficient cytoprotection to human cells in Parkinson's disease model. Angew Chem Int Edit, 2017: 14455−14459

[127]Halenova T I, Vareniuk I M, Roslova N M, *et al*. Hepatoprotective effect of orally applied water-soluble pristine C_{60} fullerene against CCl 4 -induced acute liver injury in rats. RSC Adv, 2016, **6**(102): 100046−100055

[128]Jin H, Chen W Q, Tang X W, *et al*. Polyhydroxylated C_{60}, fullerenols, as glutamate receptor antagonists and neuroprotective agents. J Neurosci Res, **62**(4): 600−607